

Local Shapley: Model-Induced Locality and Optimal Reuse in Data Valuation

Xuan Yang
Duke University
Durham, NC, USA
xuan.yang@duke.edu

Ming-Syan Chen
National Taiwan University
Taipei, Taiwan
mschen@ntu.edu.tw

Hsi-Wen Chen
National Taiwan University
Taipei, Taiwan
hwchen@arbor.ee.ntu.edu.tw

Jian Pei
Duke University
Durham, NC, USA
j.pei@duke.edu

Abstract

The Shapley value provides a principled foundation for data valuation, but exact computation is #P-hard due to the exponential coalition space. Existing accelerations remain global and ignore a structural property of modern predictors: for a given test instance, only a small subset of training points influences the prediction. We formalize this **model-induced locality** through support sets defined by the model’s computational pathway (e.g., neighbors in KNN, leaves in trees, receptive fields in GNNs), showing that Shapley computation can be projected onto these supports without loss when locality is exact. This reframes Shapley evaluation as a structured data processing problem over overlapping support-induced subset families rather than exhaustive coalition enumeration. We prove that the intrinsic complexity of Local Shapley is governed by the number of *distinct influential subsets*, establishing an information-theoretic lower bound on retraining operations. Guided by this result, we propose **LSMR** (Local Shapley via Model Reuse), an optimal subset-centric algorithm that trains each influential subset exactly once via support mapping and pivot scheduling. For larger supports, we develop **LSMR-A**, a reuse-aware Monte Carlo estimator that remains unbiased with exponential concentration, with runtime determined by the number of distinct sampled subsets rather than total draws. Experiments across multiple model families demonstrate substantial retraining reductions and speedups while preserving high valuation fidelity.

PVLDB Reference Format:

Xuan Yang, Hsi-Wen Chen, Ming-Syan Chen, and Jian Pei. Local Shapley: Model-Induced Locality and Optimal Reuse in Data Valuation. PVLDB, 14(1): XXX-XXX, 2020.
doi:XX.XX/XXX.XX

PVLDB Artifact Availability:

The source code, data, and/or other artifacts have been made available at [URL_TO_YOUR_ARTIFACTS](#).

This work is licensed under the Creative Commons BY-NC-ND 4.0 International License. Visit <https://creativecommons.org/licenses/by-nc-nd/4.0/> to view a copy of this license. For any use beyond those covered by this license, obtain permission by emailing info@vldb.org. Copyright is held by the owner/author(s). Publication rights licensed to the VLDB Endowment.

Proceedings of the VLDB Endowment, Vol. 14, No. 1 ISSN 2150-8097.
doi:XX.XX/XXX.XX

1 Introduction

Data has become a central resource for scientific discovery and commercial innovation [19, 27, 50]. As data commoditization accelerates, an increasing number of data marketplaces (e.g., Xignite, Snowflake, and Databricks) have emerged to facilitate the exchange and trading of datasets for model development across domains such as medicine, finance, and transportation [5, 13, 29, 32, 43]. Unlike traditional goods, however, the value of data is inherently context-dependent: a dataset is valuable only insofar as it improves downstream model performance. This creates a fundamental data management problem known as *data valuation*: how to rigorously quantify, attribute, and compute the contribution of individual data items to model performance in an efficient and fair manner when multiple parties jointly participate in model training [29, 43].

The Shapley value [47] provides a principled solution by assigning each data point its marginal contribution over all coalitions of the training data. It offers fairness guarantees and has become a standard foundation for data valuation [15][30]. Yet exact Shapley computation is #P-hard [26, 34] because it requires evaluating an exponential number of subsets. Existing accelerations—including Monte Carlo sampling and truncated coalition evaluation [3, 15], as well as influence- and gradient-based surrogates [1, 25, 54]—improve scalability but still operate over the *global* coalition space, implicitly assuming that every training point may affect every test point through retraining interactions (i.e., re-running the same training procedure on different data subsets).

This assumption is overly pessimistic. Modern predictors exhibit strong structural sparsity: for a fixed test instance, only a limited portion of the training data participates in the computational pathway that determines the prediction [25, 31, 46, 58]. For example, KNN predictions depend on nearby neighbors; decision trees depend on leaf-level partitions; kernel and margin-based models depend on active supports; graph neural networks depend on receptive fields [9, 16, 33, 36]. For a given test point, a large portion of training points are effectively irrelevant for that prediction. From a data management perspective, this reveals a structural opportunity: Shapley computation should exploit model-induced locality to avoid evaluating coalitions that cannot affect the outcome.

We formalize this structural sparsity as **model-induced locality**. For each test point, we define a *support set* consisting of the training instances that influence its prediction through the model’s computational graph. When this **locality** is exact, projecting the

coalition space onto the support region preserves the Shapley value. When locality is approximate, the deviation from global Shapley can be bounded by the aggregate influence of points outside the support. This reframes Shapley computation as a structured data processing problem: instead of enumerating $2^{|\mathcal{D}|}$ coalitions, we restrict attention to subsets of a much smaller support set.

However, locality alone is not sufficient. Even after restricting to supports, naïve computation remains exponential in the support size and suffers from extensive redundancy. The key insight of this paper is that the intrinsic complexity of Shapley valuation is governed not by the total number of coalitions, but by the number of *distinct subsets that influence at least one valuation*. We prove that any correct algorithm must evaluate each such subset at least once, establishing an information-theoretic lower bound on retraining complexity. This perspective shifts the problem from exponential coalition enumeration to optimal subset reuse.

Guided by this principle, we propose **LSMR** (for **Local Shapley via Model Reuse**), a subset-centric exact algorithm. LSMR builds a bipartite support-mapping graph that links subsets to the training and test points whose utilities depend on them, and applies a pivot-based scheduling rule so that each distinct subset is trained exactly once. The resulting utility is propagated to all dependent valuations. LSMR removes both intra-support and inter-support redundancy and attains the intrinsic lower bound on retraining cost.

For larger support sets where exact enumeration remains expensive, we introduce **LSMR-A**, a reuse-aware Monte Carlo estimator. Instead of treating each sampled coalition independently, LSMR-A shares every sampled subset across all compatible support sets. The estimator remains unbiased and enjoys *exponential concentration*, meaning that the probability of estimation error decreases exponentially fast with the number of samples. Importantly, its runtime depends on the number of *distinct sampled subsets* rather than the total number of draws. This decouples sampling complexity from retraining complexity and reduces variance through amortized reuse. Under *distribution shift*, when the test distribution differs from the training distribution and many training points become irrelevant to a given test instance, the variance advantage becomes *structural*: irrelevant points are never sampled, so unnecessary randomness is eliminated at its source rather than merely reduced statistically.

We evaluate our framework across four representative model families, including weighted KNN, RBF Kernel SVM, decision trees, and graph neural networks, and diverse datasets. Experiments validate the theoretical claims: support-induced locality preserves valuation fidelity; LSMR-A achieves faster convergence and dramatically reduces retraining, matching the intrinsic subset complexity.

In summary, this paper makes four main contributions. We introduce model-induced locality as a structural abstraction for data valuation, formalizing support sets and deriving bounds on the gap between global and local Shapley values. We characterize the intrinsic subset complexity induced by these supports and establish an information-theoretic lower bound on the number of retraining operations required by any correct algorithm. Guided by this principle, we propose **LSMR**, an optimal subset-centric algorithm that trains each influential subset exactly once using support mapping and pivot scheduling. Finally, we develop **LSMR-A**, a reuse-aware Monte Carlo estimator that decouples sampling from retraining,

remains unbiased with exponential concentration, and achieves lower variance through structural reuse.

The remainder of the paper is organized as follows. Section 2 reviews related work. Section 3 introduces the Local Shapley formulation and support-set abstraction. Section 4 presents the exact LSMR algorithm and proves its optimality. Section 5 develops the reuse-aware Monte Carlo estimator and its statistical guarantees. Section 6 provides an extensive empirical evaluation across multiple model families, and Section 7 concludes. The proofs of mathematical statements are provided in Appendix A.

2 Related Work

Data Valuation and Shapley-Based Methods. Data valuation [18, 22] aims to quantify the contribution of individual training examples to model performance, enabling applications such as data attribution [4], federated learning [6], model debugging [23], and dataset compression [61]. Early approaches [25] follow the leave-one-out (LOO) principle, evaluating the impact of a single training example by removing or infinitesimally perturbing it. While effective for local diagnostics, LOO-based methods do not capture interactions among training points. This limitation motivates Shapley-value-based approaches [15][48], which aggregate marginal contributions over all coalitions to provide a principled dataset-level valuation grounded in cooperative game theory.

Scalable Approximations to Shapley Values. Computing exact Shapley values is #P-hard in general [11], leading to substantial work on scalable approximations [35, 41]. Monte Carlo estimators [3, 15, 37, 52] approximate Shapley values by sampling random permutations and averaging marginal gains, while reinforcement-learning-based methods [59] learn sampling policies to avoid exhaustive enumeration. Other approaches exploit structural properties of learning algorithms to reduce retraining costs, including convexity [21], submodularity [57], and influence-function-based reuse of gradients or Hessians [1, 44]. Despite these advances, existing methods largely operate over the full global coalition space. Even when computational shortcuts are employed, they do not explicitly leverage model-induced sparsity in the prediction pathway of individual test points. In particular, prior work does not characterize the intrinsic subset complexity induced by structural locality, nor does it establish lower bounds on the number of distinct retraining operations required for correct Shapley computation.

Locality-Aware Shapley Computation. Motivated by the inefficiency of global coalition enumeration, several recent works explore locality-aware Shapley evaluation. For unweighted KNN classifiers, Jia et al. [20] observe that prediction at a test point depends primarily on its nearest neighbors and show that ignoring distant points preserves relative importance rankings, enabling efficient approximate local Shapley computation. Wang et al. [53] extend this idea to hard-label KNN via dynamic programming, and Zhang et al. [60] propose a near-linear-time weighted KNN-Shapley algorithm using a duplication trick. These methods demonstrate the practical benefit of restricting computation to local neighborhoods. However, their notion of locality is geometric and specific to KNN models. They do not generalize beyond distance-based neighborhoods, nor do they formalize locality as a structural property of the model’s computational pathway.

Comparison with Prior Work. In contrast, we introduce *model-induced support sets* that abstract locality directly from the architecture and prediction mechanism of the model. This formulation applies to a broader class of predictors, including margin-based models, decision trees, kernel methods, and graph neural networks. Furthermore, we characterize the intrinsic family of distinct subsets induced by these supports and prove that any correct algorithm must evaluate each such subset at least once, establishing an information-theoretic lower bound on retraining complexity. Building on this structural perspective, we develop both an exact reuse algorithm (LSMR) and a reuse-aware Monte Carlo estimator (LSMR-A) that decouple sampling complexity from retraining complexity. This unified treatment of locality, subset reuse, and optimal retraining distinguishes our approach from prior locality-aware and approximation-based methods.

3 Local Shapley

We first review the standard Shapley value for data valuation, then introduce a localized variant that restricts computation to training points relevant to a given test prediction. Finally, we discuss how this locality notion extends across different model families. Appendix A.1 summarizes frequently used notations.

3.1 Shapley Value for Data Valuation

Let \mathcal{D} denote a training dataset, where each data point is $z = (\mathbf{x}_z, y_z)$ with feature vector \mathbf{x}_z and class label y_z . Data valuation [15] seeks to quantify how much each training point contributes to predictive performance on a testing set \mathcal{T} . Formally, we aim to construct a valuation function $\phi : \mathcal{D} \rightarrow \mathbb{R}$ that assigns an importance score to every $z \in \mathcal{D}$.

Utility induced by retraining. For each test point $t \in \mathcal{T}$, we define a utility function $v_t : 2^{\mathcal{D}} \rightarrow \mathbb{R}$, where $v_t(S)$ measures the performance of a model trained on a subset $S \subseteq \mathcal{D}$ when evaluated at t . Throughout the paper, we adopt the standard retraining-based formulation as follows

$$v_t(S) = g_t(\theta(S)), \quad (1)$$

where $\theta(S)$ denotes the model parameters obtained by training on S , and $g_t(\cdot)$ is a scalar evaluation functional at test point t . Examples include prediction confidence [20], signed margin [25], and loss reduction [15]. We assume that model hyperparameters and training procedures are fixed across coalitions, so that variation in $v_t(S)$ arises solely from the choice of training subset S . In the computational model considered throughout this work, the dominant cost of evaluating $v_t(S)$ is the training step required to obtain $\theta(S)$.

Global Shapley value. The Shapley value [47] assigns to each training point its average marginal contribution over all possible coalitions. For a fixed test point t and training point $z \in \mathcal{D}$, the Shapley value is

$$\phi_z(v_t) = \frac{1}{|\mathcal{D}|} \sum_{S \subseteq \mathcal{D} \setminus \{z\}} \frac{v_t(S \cup \{z\}) - v_t(S)}{\binom{|\mathcal{D}|-1}{|S|}}. \quad (2)$$

Equivalently, $\phi_z(v_t)$ is the expected marginal gain of z under a uniformly random permutation of \mathcal{D} , and it satisfies the classical axioms of efficiency, symmetry, null player, and additivity [47].

When multiple test points are considered, we aggregate per-test-point values additively:

$$\phi_z = \sum_{t \in \mathcal{T}} \phi_z(v_t). \quad (3)$$

This summation corresponds to evaluating total contribution over \mathcal{T} . By linearity of the Shapley value [34], analysis can be conducted independently for each test point and combined afterward. Accordingly, we focus on a single fixed t in the sequel.

Computational barrier and structural redundancy. Computing $\phi_z(v_t)$ requires evaluating marginal contributions over all $2^{|\mathcal{D}|}$ subsets of \mathcal{D} . Since each evaluation involves retraining the model on S to obtain $\theta(S)$, exact computation is computationally prohibitive. In fact, computing the Shapley value of a single player in a general cooperative game is #P-hard [11].

Crucially, the classical formulation treats every training point as potentially influential for every test point across all coalitions. That is, the global coalition space $2^{\mathcal{D}}$ implicitly assumes that influence may propagate arbitrarily through retraining. However, modern learning architectures often exhibit strong structural sparsity: for a fixed test point t , only a small portion of the training data meaningfully participates in the computational pathway that determines $v_t(S)$. This observation suggests that the global coalition space contains substantial structural redundancy. The next subsection formalizes this idea by introducing a localized utility that restricts attention to the subset of training points relevant to t , leading to the notion of *Local Shapley value*.

3.2 Local Shapley Value

The classical Shapley formulation implicitly treats every training point as potentially influential for every test point across all coalitions. However, modern learning systems often exhibit strong *structural locality*: for a fixed test point t , only a limited portion of the training data participates in the computational pathway that determines $v_t(S)$. This observation suggests that the global coalition space $2^{\mathcal{D}}$ contains substantial redundancy when evaluating the contribution of training data to t .

Support sets as structural locality. To formalize this idea, we introduce a *support set* $\mathcal{N}(t) \subseteq \mathcal{D}$, defined as the subset of training points that can meaningfully influence the prediction or utility at t . The support set may be determined by architectural structure (e.g., receptive fields in GNNs, leaf membership in trees), margin sparsity (e.g., support vectors), kernel bandwidth, or other model-specific mechanisms. We treat $\mathcal{N}(t)$ as fixed with respect to a reference model trained once on the full dataset, so that locality reflects structural dependency rather than coalition-dependent drift. Its size can be controlled via model hyperparameters (e.g., K in KNN [10], threshold in kernel methods [42], hop radius in GNN [24]), thereby trading fidelity for efficiency.

We define the *projected (local) utility* as follows.

$$v_t^{\mathcal{N}}(S) := v_t(S \cap \mathcal{N}(t)), \quad \forall S \subseteq \mathcal{D}. \quad (4)$$

Since $v_t^{\mathcal{N}}(S)$ depends only on $S \cap \mathcal{N}(t)$, coalitions that agree on their intersection with $\mathcal{N}(t)$ are indistinguishable under the projected utility. Consequently, the cooperative game induced by $v_t^{\mathcal{N}}$ is effectively defined on the $2^{|\mathcal{N}(t)|}$ subsets of the support set, and

players outside $\mathcal{N}(t)$ do not enlarge the intrinsic coalition space (formalized in Lemma 1).

Definition 1 (Local Shapley Value). *For a training point $z \in \mathcal{D}$, the local Shapley value with respect to test point t is defined as the classical Shapley value computed under the projected utility v_t^N :*

$$\phi_z^{\text{loc}}(v_t) = \frac{1}{|\mathcal{D}|} \sum_{S \subseteq \mathcal{D} \setminus \{z\}} \frac{v_t^N(S \cup \{z\}) - v_t^N(S)}{\binom{|\mathcal{D}|-1}{|S|}}. \quad (5)$$

From Eq. (4), if $z \notin \mathcal{N}(t)$, then $v_t^N(S \cup \{z\}) = v_t^N(S)$ for all S , so z acts as a null player and $\phi_z^{\text{loc}}(v_t) = 0$. For $z \in \mathcal{N}(t)$, the valuation depends only on coalitions formed within the support set.

When does locality approximate the global game? Local projection modifies the cooperative game by removing non-support players. To quantify the resulting approximation error, we impose a stability condition controlling how non-local points affect marginal contributions.

Assumption 1 (Additive Non-local Stability). *Given a test point t , for any $z \in \mathcal{N}(t)$, there exist nonnegative constants $\{\ell_{t,z}(u)\}_{u \in \mathcal{D} \setminus \mathcal{N}(t)}$ such that for any $S \subseteq \mathcal{N}(t) \setminus \{z\}$ and any $U \subseteq \mathcal{D} \setminus \mathcal{N}(t)$,*

$$|\Delta_z v_t(S \cup U) - \Delta_z v_t(S)| \leq \sum_{u \in U} \ell_{t,z}(u),$$

where $\Delta_z v_t(S) := v_t(S \cup \{z\}) - v_t(S)$. \square

This assumption formalizes a structural locality principle: non-support points influence the marginal effect of z only weakly, and their aggregate impact scales at most additively [55]. It is usually satisfied by stable learning algorithms [25] in which parameter perturbations caused by inserting a data point decay with coalition size.

Proposition 1 (Approximation of Global Shapley). *Under Assumption 1, for any $z \in \mathcal{N}(t)$,*

$$|\phi_z(v_t) - \phi_z^{\text{loc}}(v_t)| \leq \frac{1}{2} \sum_{u \in \mathcal{D} \setminus \mathcal{N}(t)} \ell_{t,z}(u),$$

where $\phi_z(v_t)$ denotes the global Shapley value computed under the original utility v_t . \square

Using the permutation interpretation of the Shapley value, a non support point influences the marginal contribution of z only when it appears before z in a uniformly random ordering, which happens with probability one half. Invoking Assumption 1 together with the bound established in the proposition above, the deviation between the global and local valuations is controlled by one half of the total non local interaction mass. The approximation error therefore depends only on the aggregate strength of interactions outside the support, rather than on the size of the full training set. Hence, whenever such effects decay with distance, kernel bandwidth, or graph hop radius, a moderately sized support set is sufficient to maintain valuation fidelity.

Example of regularized ERM. Consider ℓ_2 -regularized empirical risk minimization

$$F_S(w) = \frac{1}{|S|} \sum_{i \in S} f_i(w) + \frac{\lambda}{2} \|w\|_2^2,$$

where each f_i is convex and L -smooth. Then F_S is λ -strongly convex, and classical stability analysis [25] yields

$$\|w_{S \cup \{u\}} - w_S\|_2 = O\left(\frac{1}{\lambda|S|}\right).$$

If the evaluation functional $g_t(w)$ is ψ -Lipschitz in w , then

$$|v_t(S \cup \{u\}) - v_t(S)| = O\left(\frac{\psi}{\lambda|S|}\right).$$

Moreover, the interaction term

$$|\Delta_z v_t(S \cup \{u\}) - \Delta_z v_t(S)| = O\left(\frac{1}{\lambda|S|^2}\right)$$

(up to alignment factors), which satisfies Assumption 1, where $\ell_{t,z}(u)$ decays rapidly as shown in Proposition 1. Consequently, the total non-local influence $\sum_{u \notin \mathcal{N}(t)} \ell_{t,z}(u)$ remains small when interactions are weak.

Axiomatic properties. An important question is whether restricting the game to the support set preserves the fundamental fairness guarantees of the Shapley framework.

Proposition 2 (Properties of Local Shapley). *The local Shapley value satisfies: (i) **Symmetry**: identically contributing data points receive equal value; (ii) **Null Player**: a data point with zero marginal contribution in all coalitions receives zero value; and (iii) **Additivity**: the valuation is linear in v_t .*

Since $\phi_z^{\text{loc}}(v_t)$ is the classical Shapley value applied to the projected utility v_t^N , it satisfies symmetry, null-player, and additivity. Efficiency holds with respect to the projected utility v_t^N ; relative to the original utility v_t , any deviation from global efficiency corresponds precisely to the total utility mass discarded by excluding points outside $\mathcal{N}(t)$. When locality is exact (e.g., Threshold KNN [8]), we have $v_t^N = v_t$, and efficiency holds with respect to the original utility as well.

Discussion and limitations. Locality is structural rather than universal. Highly nonconvex models with strong global parameter coupling may violate Assumption 1, leading to larger approximation gaps. In such regimes, $\mathcal{N}(t)$ should be enlarged to capture long-range interactions. The framework therefore provides a tunable spectrum between global fidelity and computational tractability.

3.3 Locality Induced by Model Architecture

Section 3.2 introduced the abstract support set $\mathcal{N}(t)$ and showed that, whenever the prediction at t depends only on this subset (exactly or approximately), the effective cooperative game collapses from $2^{|\mathcal{D}|}$ to $2^{|\mathcal{N}(t)|}$. We now demonstrate that such support sets arise naturally in common model families as a consequence of their computational structure. In some cases locality is exact and Local Shapley coincides with the global Shapley value; in others locality is approximate but satisfies Assumption 1, yielding controlled error.

Remark 1 (Architectural Sources of Locality). *In many widely used predictors, the prediction at t depends only on a structurally determined subset $\mathcal{N}(t) \subseteq \mathcal{D}$:*

- (1) **KNN models** [10, 12]: *The prediction is computed solely from the K nearest neighbors of t , so $\mathcal{N}(t)$ is naturally defined as this K -point neighborhood. Locality is determined by Euclidean distance and is exact under the threshold setting [56].*
- (2) **Support vector machines** [7, 9]: *The prediction admits a sparse dual form involving only support vectors, i.e., $\mathcal{N}(t) = \{z \in \mathcal{D} : \alpha_z \neq 0\}$. Locality is representational: although parameters are trained globally, only support vectors influence predictions.*

- (3) **Kernel methods with compact support** [40, 42]: For kernels with finite bandwidth, only training points satisfying $\|x_z - x_t\| \leq h$ contribute, yielding $\mathcal{N}(t) = \{z \in \mathcal{D} : \|x_z - x_t\| \leq h\}$. Locality is governed by bandwidth.
- (4) **Decision trees** [2, 45]: The prediction at t is determined by the leaf reached along its decision path. The relevant training points are those passing through the same parent node, and we define $\mathcal{N}(t) = \{z \in \mathcal{D} : z \text{ reaches the same parent node as } t\}$. Locality arises from rule-based partitioning of the input space.
- (5) **Graph neural networks** [16, 17, 24]: In a L -layer message-passing GNN, only nodes within the L -hop receptive field of t directly influence its embedding, so $\mathcal{N}(t)$ is the L -hop neighborhood of t . Locality is structural and induced by graph topology.

Across these families, locality emerges through distinct architectural mechanisms: geometric proximity (KNN), dual sparsity (SVM), finite bandwidth (compact kernels), rule-based partitioning (trees), and graph message passing (GNNs). In each case, $\mathcal{N}(t)$ is determined by the computational pathway that produces the prediction at t , and typically satisfies $|\mathcal{N}(t)| \ll |\mathcal{D}|$. When this dependency is strictly finite, Local Shapley recovers the global Shapley value exactly; when influence decays but is not strictly zero, the approximation gap is governed by the aggregate non-local interaction mass characterized in Proposition 1. These examples show that locality is a structural property of modern predictors, providing a principled and model-agnostic foundation for local Shapley analysis.

4 Exact Algorithm for Local Shapley

Building on the Local Shapley formulation in Section 3.2, we now turn to exact computation. Although Definition 1 replaces the original utility with the projected utility $v_t^{\mathcal{N}}$, its combinatorial form still formally ranges over all $2^{|\mathcal{D}|}$ coalitions. We first prove that the projected utility induces an equivalent cooperative game whose effective player set is the support set $\mathcal{N}(t)$, thereby collapsing the intrinsic coalition space from $2^{|\mathcal{D}|}$ to $2^{|\mathcal{N}(t)|}$.

This dimensional reduction alone, however, does not eliminate computational redundancy. A naïve local evaluation still enumerates all subsets of $\mathcal{N}(t)$ separately for each training and test point. As shown in Figure 1, two inefficiencies remain: *intra-support redundancy*, where training points within the same support set require repeated evaluation of identical subsets, and *inter-support redundancy*, where overlapping support sets across test points trigger duplicate subset retraining. In this section, we eliminate these redundancies in a structured manner: first by reorganizing the Shapley computation around subsets rather than players, and then by introducing a global reuse mechanism that guarantees each distinct subset is trained once while preserving exactness.

4.1 Reducing the Game to the Support Set

We begin by formalizing the intrinsic dimensional reduction induced by the projected utility. Although Definition 1 is written over subsets of the full dataset \mathcal{D} , the projected utility satisfies $v_t^{\mathcal{N}}(S) = v_t(S \cap \mathcal{N}(t))$, implying that coalitions that agree on their intersection with $\mathcal{N}(t)$ are indistinguishable. Consequently, the Shapley computation for test point t depends only on subsets of the support set $\mathcal{N}(t)$.

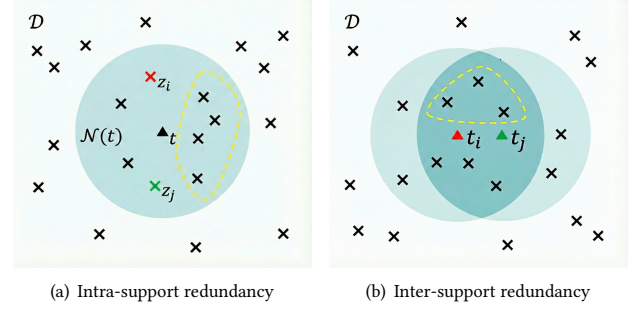


Figure 1: (a) *Intra-support redundancy*: the blue area denotes the support set $\mathcal{N}(t)$. For training points z_i and z_j , many training subsets are shared in their Shapley value computations. (b) *Inter-support redundancy*: test points t_i and t_j have overlapping supports (darker blue). Within this overlap, subsets are shared across their Shapley computations. The yellow dotted subset illustrates one such shared training subset.

Algorithm 1 Baseline Algorithm

Require: Training set \mathcal{D} , test set \mathcal{T}

Ensure: Local Shapley value ϕ_z for each $z \in \mathcal{D}$

- 1: **for** each $z \in \mathcal{D}$ **do**
 - 2: initialize $\phi_z \leftarrow 0$
 - 3: **for** each test point $t \in \mathcal{T}$ **do**
 - 4: Retrieve support set $\mathcal{N}(t)$
 - 5: **for** each training point $z \in \mathcal{N}(t)$ **do**
 - 6: **for** each subset $S \subseteq \mathcal{N}(t) \setminus \{z\}$ **do**
 - 7: Train model $\theta(S)$ and evaluate $v_t(S)$;
 - 8: Train model $\theta(S \cup \{z\})$ and evaluate $v_t(S \cup \{z\})$;
 - 9: $\phi_z \leftarrow \phi_z + \frac{v_t(S \cup \{z\}) - v_t(S)}{|\mathcal{N}(t)| \cdot \binom{|\mathcal{N}(t)|-1}{|S|}}$.
 - 10: **return** $\{\phi_z : z \in \mathcal{D}\}$
-

Lemma 1 (Equivalence Under Projected Utility). *The local Shapley value in Definition 1, can be equivalently expressed as*

$$\phi_z^{\text{loc}}(v_t) = \frac{1}{|\mathcal{N}(t)|} \sum_{S \subseteq \mathcal{N}(t) \setminus \{z\}} \frac{v_t(S \cup \{z\}) - v_t(S)}{\binom{|\mathcal{N}(t)|-1}{|S|}}. \quad \square$$

Lemma 1 shows that the Local Shapley value for t can be computed by treating $\mathcal{N}(t)$ as the effective player set. Thus, the intrinsic coalition space collapses from $2^{|\mathcal{D}|}$ to $2^{|\mathcal{N}(t)|}$. For subsets of size k , there are $\binom{|\mathcal{N}(t)|}{k}$ coalitions. Since each marginal contribution requires evaluating both $v(S)$ and $v(S \cup \{z\})$, direct enumeration over the reduced space yields the training cost as follows.

$$2 \sum_{k=1}^{|\mathcal{N}(t)|} k \binom{|\mathcal{N}(t)|}{k} = |\mathcal{N}(t)| \cdot 2^{|\mathcal{N}(t)|} \quad (6)$$

Aggregating over all test points, the total number of evaluations becomes

$$\sum_{t \in \mathcal{T}} |\mathcal{N}(t)| \cdot 2^{|\mathcal{N}(t)|}, \quad (7)$$

which is much smaller than the $|\mathcal{T}| \cdot |\mathcal{D}| \cdot 2^{|\mathcal{D}|}$ cost of global Shapley when $|\mathcal{N}(t)| \ll |\mathcal{D}|$. This serves as the natural local baseline and is summarized in Algorithm 1.

4.2 Subset-Centric Reformulation: Eliminating Intra-Support Redundancy

The baseline local strategy still evaluates marginal contributions separately for each training point in $\mathcal{N}(t)$. As a result, identical subsets are repeatedly trained when computing Shapley values for different players within the same support set. To remove this intra-support redundancy, we reorganize the computation around subsets rather than individual players.

Lemma 2 (Subset-Centric Reformulation). *For any test point t and training point $z \in \mathcal{N}(t)$, the local Shapley value admits the following equivalent expression:*

$$\phi_z^{\text{loc}}(v_t) = \frac{1}{|\mathcal{N}(t)|} \sum_{S \subseteq \mathcal{N}(t)} \frac{(-1)^{\mathbb{I}(z \notin S)} v_t(S)}{\binom{|\mathcal{N}(t)|-1}{|S|-\mathbb{I}(z \in S)}}. \quad \square$$

Lemma 2 expresses the Local Shapley value as a weighted sum over all subsets $S \subseteq \mathcal{N}(t)$, where the contribution of each subset depends only on whether a training point z belongs to S . Thus, a single evaluation of $v_t(S)$ simultaneously updates the Shapley values of all $z \in \mathcal{N}(t)$: subsets containing z correspond to coalitions after including z and contribute positively, while subsets excluding z correspond to coalitions before adding z and contribute negatively, with weights given in closed form.

This reformulation yields an immediate computational improvement. Instead of evaluating marginal contributions separately for each $z \in \mathcal{N}(t)$ over all subsets $S \subseteq \mathcal{N}(t) \setminus \{z\}$, which requires $|\mathcal{N}(t)| \cdot 2^{|\mathcal{N}(t)|}$ utility evaluations per test point, we now evaluate only the $2^{|\mathcal{N}(t)|}$ distinct subsets of the support set and distribute their contributions algebraically. Consequently, intra-support redundancy is eliminated and the per-test-point cost is reduced by a factor of $|\mathcal{N}(t)|$.

At this point, the computation is localized to $\mathcal{N}(t)$ and reorganized in a subset-centric manner, eliminating redundancy within each support set. Nevertheless, subsets that appear in overlapping supports of different test points are still evaluated independently. The next subsection addresses this remaining inefficiency by introducing a global reuse mechanism that ensures each distinct subset is trained only once across all test points.

4.3 Global Subset Reuse Across Test Points

While each subset $S \subseteq \mathcal{N}(t)$ is now evaluated only once per test point, overlapping support sets across \mathcal{T} can still trigger repeated retraining of the identical subset. Because computing $v_t(S)$ requires training $\theta(S)$ —the dominant cost—such duplication significantly inflates runtime. We therefore develop a global reuse strategy that canonicalizes subset evaluation across test points.

To eliminate this remaining redundancy, we introduce **Local Shapley via Model Reuse (LSMR)**, which ensures that every distinct subset S is trained exactly once across the entire computation and reused wherever it is valid. The key principle is global subset canonicalization: each subset has a unique designated evaluator, and all other occurrences reuse its result. LSMR achieves this through three components: a bipartite support-mapping graph, reverse support-set indexing, and pivot-based scheduling.

4.3.1 Global Support Structure We represent training–test dependencies using a bipartite structure $G = (\mathcal{D}, \mathcal{T}, \mathcal{N}, \mathcal{R})$, where $\mathcal{N}(t) \subseteq$

Algorithm 2 LSMR

```

1: Input: Bipartite support-mapping structure  $G = (\mathcal{D}, \mathcal{T}, \mathcal{N}, \mathcal{R})$ , or-
   ordered test set  $\Pi_{\mathcal{T}}$ 
2: Output: Local Shapley values  $\phi_z$  for each  $z \in \mathcal{D}$ 
3: Initialize  $\phi_z \leftarrow 0$  for all  $z \in \mathcal{D}$ 
4: for all test point  $t \in \mathcal{T}$  in order  $\Pi_{\mathcal{T}}$  do
5:   Retrieve support set  $\mathcal{N}(t)$  from  $G$ 
6:   for all subsets  $S \subseteq \mathcal{N}(t)$  do
7:     if  $S = \emptyset$  then
8:        $\mathcal{R}_S \leftarrow \mathcal{T}$ 
9:     else
10:       $\mathcal{R}_S \leftarrow \bigcap_{z \in S} \mathcal{R}(z)$ 
11:     $t^* \leftarrow$  first test point in  $\mathcal{R}_S$  under  $\Pi_{\mathcal{T}}$ 
12:    if  $t = t^*$  then
13:      Train model  $\theta(S)$  and evaluate  $v_{t^*}(S)$  for all  $t' \in \mathcal{R}_S$ 
14:      for all  $t' \in \mathcal{R}_S$  do
15:        for all  $z \in \mathcal{N}(t')$  do
16:          if  $z \in S$  then
17:             $\phi_z \text{ += } \frac{v_{t'}(S)}{|\mathcal{N}(t')| \cdot \binom{|\mathcal{N}(t')|-1}{|S|-1}}$ 
18:          else
19:             $\phi_z \text{ -= } \frac{v_{t'}(S)}{|\mathcal{N}(t')| \cdot \binom{|\mathcal{N}(t')|-1}{|S|}}$ 
20: return  $\{\phi_z : z \in \mathcal{D}\}$ 

```

\mathcal{D} is the support of test point t , and

$$\mathcal{R}(z) = \{t \in \mathcal{T} : z \in \mathcal{N}(t)\} \quad (8)$$

is the reverse map listing the test points whose supports contain training point z . The mappings \mathcal{N} and \mathcal{R} are relational inverses, and together they characterize all potential reuse opportunities across test points.

4.3.2 Reverse Support-Set Indexing For any subset $S \subseteq \mathcal{D}$, only test points whose supports contain S can reuse its evaluation. These test points are exactly

$$\mathcal{R}_S = \bigcap_{z \in S} \mathcal{R}(z), \quad \mathcal{R}_{\emptyset} = \mathcal{T}. \quad (9)$$

Thus, \mathcal{R}_S enumerates all test points for which $S \subseteq \mathcal{N}(t)$. Computing \mathcal{R}_S requires intersecting adjacency lists, whose cost is negligible compared to model retraining because supports are typically small and sparse.

4.3.3 Pivot-Based Scheduling To guarantee uniqueness, LSMR assigns each subset S a canonical evaluator. Fix a global ordering $\Pi_{\mathcal{T}}$ over test points and define the pivot

$$t^*(S) = \arg \min_{t' \in \mathcal{R}_S} \Pi_{\mathcal{T}}(t'). \quad (10)$$

Subset S is trained only when processing its pivot $t^*(S)$. For any other $t' \in \mathcal{R}_S$, the subset has already been evaluated at its pivot and the result is reused. This rule ensures that each distinct subset is trained exactly once, eliminating all inter-support redundancy.

4.3.4 Complete LSMR Procedure Combining subset-centric reformulation with global reuse yields a unified pipeline. For each test point t , LSMR enumerates all subsets $S \subseteq \mathcal{N}(t)$. When encountering S , the algorithm computes \mathcal{R}_S and checks whether t is the pivot $t^*(S)$. If so, it trains $\theta(S)$, evaluates $v_{t^*}(S)$ for all $t' \in \mathcal{R}_S$ and redistributes the utility values to all $z \in \mathcal{N}(t')$ using the closed-form

weights from Lemma 2; otherwise, the subset has already been processed and no retraining occurs.

By construction, LSMR removes both intra-support redundancy (via subset-centric reformulation) and inter-support redundancy (via global pivot reuse), ensuring that each distinct subset S is trained exactly once while preserving exact Local Shapley values.

4.4 Optimality and Complexity Analysis

We now quantify the computational savings of global subset reuse. Since the dominant cost is model retraining, we measure complexity by counting the number of distinct subsets S for which $\theta(S)$ must be trained. Let

$$\mathcal{S} = \bigcup_{t \in \mathcal{T}} \{S \subseteq \mathcal{N}(t)\} \quad (11)$$

denote the family of all distinct subsets that appear across support sets. The size $|\mathcal{S}|$ thus reflects the intrinsic retraining complexity of the Local Shapley problem under a given support mapping.

Theorem 1 (Optimal Reuse). *Let \mathcal{R}_S be the set of test points whose support sets contain S . Any algorithm computing $\{v_t(S)\}_{t \in \mathcal{R}_S}$ must evaluate $v(S)$ at least once for every $S \in \mathcal{S}$.*

Theorem 1 shows that any correct algorithm must evaluate each subset in \mathcal{S} at least once. Thus $|\mathcal{S}|$ is an information-theoretic lower bound on the number of model trainings. By construction, LSMR attains this bound exactly, performing one training per distinct subset and no more. By definition, we have

$$|\mathcal{S}| \leq \min \left\{ \sum_{t \in \mathcal{T}} 2^{|\mathcal{N}(t)|}, 2^{|\mathcal{D}|} \right\}. \quad (12)$$

The first term corresponds to independently enumerating all subsets within each support set, while the second reflects the trivial upper bound over the entire dataset. In contrast, LSMR performs exactly $|\mathcal{S}|$ trainings, which can be substantially smaller when supports overlap. We therefore conclude across four levels of evaluation:

- **Global Shapley:** $|\mathcal{T}| \cdot |\mathcal{D}| \cdot 2^{|\mathcal{D}|}$ trainings.
- **Local baseline:** $\sum_{t \in \mathcal{T}} |\mathcal{N}(t)| \cdot 2^{|\mathcal{N}(t)|}$ trainings.
- **Subset-centric:** $\sum_{t \in \mathcal{T}} 2^{|\mathcal{N}(t)|}$ trainings.
- **LSMR:** $|\mathcal{S}|$ trainings.

The final quantity depends only on the number of *distinct* subsets induced by all supports, not on the number of test points or the number of players per support.

In practical regimes where test points are drawn from a fixed distribution, supports induced by nearby test points tend to overlap significantly. As $|\mathcal{T}|$ grows, many new test points introduce no new subsets, and the growth of $|\mathcal{S}|$ is sublinear relative to $\sum_{t \in \mathcal{T}} 2^{|\mathcal{N}(t)|}$. Consequently, the amortized number of model trainings per test point decreases with scale, making LSMR particularly effective in large evaluation settings.

Corollary 1 (Amortized Reuse). *Assume the support mapping $\mathcal{N}(\cdot)$ has finite range, i.e., only finitely many distinct support sets can appear across test points. Let $\mathcal{S}_T = \bigcup_{t \in \mathcal{T}_T} \{S \subseteq \mathcal{N}(t)\}$ denote the family of distinct subsets induced by the first T test points. Then $|\mathcal{S}_T|$ is bounded while T increases, and consequently $\frac{|\mathcal{S}_T|}{T} \rightarrow 0$ as $T \rightarrow \infty$. Therefore, the amortized number of model trainings per test point under LSMR vanishes as T grows. \square*

5 Monte Carlo Approximation for Local Shapley

While LSMR is optimal for exact evaluation, it still requires enumerating all $2^{|\mathcal{N}(t)|}$ subsets, which becomes impractical when $|\mathcal{N}(t)|$ is large. For stochastic approximation, classical Monte Carlo methods [39] estimate Shapley values by sampling permutations and averaging marginal contributions to avoid exhaustive enumeration. However, standard MC is *player-centric*, retraining each sampled coalition independently and repeatedly, failing to exploit the structural reuse opportunities identified in Section 4.3. This motivates a reuse-aware Monte Carlo strategy.

5.1 From Exact Reuse to Reuse-Aware Sampling

We therefore develop **LSMR-A**, a stochastic estimator that integrates the subset-centric formulation and pivot-based canonicalization of LSMR into the Monte Carlo setting. The resulting algorithm preserves unbiasedness and concentration guarantees while ensuring that each distinct subset is trained at most once across all samples and test points.

5.1.1 Subset-Centric Monte Carlo Estimation Standard permutation-based MC estimates the Shapley value of a player z by averaging marginal gains $v_t(S \cup \{z\}) - v_t(S)$ over sampled subsets S . This formulation ties each sample to a specific player, making cross-player reuse impossible. In contrast, Lemma 2 expresses the Local Shapley value as a weighted expectation over subsets $S \subseteq \mathcal{N}(t)$. This observation enables a conceptual shift from a marginal-gain estimator to a *subset-centric weighted utility estimator*. Instead of associating each sample with a single player, LSMR-A samples subsets S and updates the Shapley values of *all* players in $\mathcal{N}(t)$ simultaneously using the closed-form weights derived in Lemma 2.

Under this formulation, a single model training on S becomes a shared computational resource for the entire support set, eliminating intra-support redundancy in the stochastic setting.

5.1.2 Pivoted Sampling for Cross-Test Reuse To extend reuse across test points, we integrate the pivot mechanism introduced in Section 4.3. For each test point t , LSMR-A draws M random permutations of $\mathcal{N}(t)$ and extracts the prefix-before- t subset S in the standard Shapley sampling manner.

For a sampled subset S , only test points whose supports contain S can reuse its evaluation. These are precisely the elements of \mathcal{R}_S . To keep the estimator unbiased, we assign each subset a canonical evaluator via the pivot rule as follows.

$$t^*(S) = \arg \min_{t' \in \mathcal{R}_S} \Pi_{\mathcal{T}}(t'). \quad (13)$$

The sampling procedure follows two cases:

- **Pivot hit:** If the current test point t equals $t^*(S)$, the subset is accepted. The model $\theta(S)$ is trained once and reused to evaluate $v_{t'}(S)$ for all $t' \in \mathcal{R}_S$. These utilities are distributed to all $z \in \mathcal{N}(t')$ using the weighted subset-centric update rule.
- **Pivot miss:** If $t \neq t^*(S)$, the sample is discarded. Since S is assigned exclusively to its pivot $t^*(S)$, discarding avoids duplicate retraining without altering the sampling distribution.

This pivoted sampling scheme ensures that each distinct subset S is trained at most once across all samples and test points, while preserving the unbiasedness of the estimator. The complete procedure is summarized in Algorithm 3.

Algorithm 3 LSMR-A

```

1: Input: Bipartite support-mapping structure  $G = (\mathcal{D}, \mathcal{T}, \mathcal{N}, \mathcal{R})$ , ordered test set  $\Pi_{\mathcal{T}}$ , number of Monte Carlo samples  $M$ 
2: Output: Local Shapley values  $\phi_z$  for each  $z \in \mathcal{D}$ 
3: Initialize  $\phi_z \leftarrow 0$  for all  $z \in \mathcal{D}$ 
4: for all test point  $t \in \mathcal{T}$  in order  $\Pi_{\mathcal{T}}$  do
5:   Retrieve support set  $\mathcal{N}(t)$  from  $G$ 
6:   for  $m = 1$  to  $M$  do
7:     Sample a random permutation  $\pi$  of  $\mathcal{N}(t) \cup \{t\}$ 
8:     Let  $i$  be the position of  $t$  in  $\pi$ 
9:     Define subset  $S \leftarrow \{\pi_1, \dots, \pi_{i-1}\}$ 
10:    if  $S = \emptyset$  then
11:       $\mathcal{R}_S \leftarrow \mathcal{T}$ 
12:    else
13:       $\mathcal{R}_S \leftarrow \bigcap_{z \in S} \mathcal{R}(z)$ 
14:     $t^* \leftarrow$  first test point in  $\mathcal{R}_S$  under  $\Pi_{\mathcal{T}}$ 
15:    if  $t = t^*$  then
16:      Train model  $\theta(S)$  and evaluate  $v_{t'}(S)$  for all  $t' \in \mathcal{R}_S$ 
17:      for all  $t' \in \mathcal{R}_S$  do
18:        for all  $z \in \mathcal{N}(t')$  do
19:          if  $z \in S$  then
20:             $\phi_z \text{ += } \frac{(|\mathcal{N}(t')| + 1) \cdot v_{t'}(S)}{|S| \cdot M}$ 
21:          else
22:             $\phi_z \text{ -= } \frac{(|\mathcal{N}(t')| + 1) \cdot v_{t'}(S)}{(|\mathcal{N}(t')| - |S|) \cdot M}$ 
23: return  $\{\phi_z : z \in \mathcal{D}\}$ 

```

5.2 Statistical Guarantees

We first analyze the statistical validity and convergence properties of LSMR-A. The resulting guarantees mirror classical Monte Carlo analysis, while incorporating the effect of pivot-based reuse. We begin by establishing unbiasedness in expectation.

Theorem 2 (Unbiasedness of LSMR-A). *For each test point $t \in \mathcal{T}$, let $\ell_t = |\mathcal{N}(t)|$. In each Monte Carlo round, LSMR-A draws a uniform permutation of $\mathcal{N}(t) \cup \{t\}$ and takes the prefix-before- t subset S . The pivot associated with S is the first test point in the fixed ordering $\Pi_{\mathcal{T}}$, denoted $t^*(S)$. The model is trained on S only when processing $t = t^*(S)$, and the resulting utilities $v_{t'}(S)$ are reused for all t' such that $S \subseteq \mathcal{N}(t')$. Under this reuse mechanism, a MC estimator satisfies*

$$\mathbb{E}[\widehat{\phi}(z)] = \sum_{t \in \mathcal{T}} \frac{\mathbb{I}(z \in \mathcal{N}(t))}{|\mathcal{N}(t)|} \sum_{S \subseteq \mathcal{N}(t)} \frac{(-1)^{\mathbb{I}(z \notin S)} v_t(S)}{\binom{|\mathcal{N}(t)|-1}{|S|-\mathbb{I}(z \in S)}},$$

which coincides exactly with the closed-form Local Shapley value. Thus, LSMR-A is an unbiased estimator. \square

The estimator remains unbiased because each subset S is drawn from the same permutation-induced distribution as in classical MC, and the pivot rule merely canonicalizes which test point evaluates it. The weighted subset-centric update from Lemma 2 preserves the exact expectation of the Local Shapley value.

We then prove exponential concentration of the estimator around the true Local Shapley value. The guarantee follows from independent permutation sampling together with standard bounded-difference inequalities.

Theorem 3 (Concentration of LSMR-A). *Assume $|v_t(S)| \leq B$ for all t and all subsets S . Let $\widehat{\phi}(z)$ be the estimator obtained from M*

samples. Then for any $\epsilon > 0$,

$$\Pr\left(|\widehat{\phi}(z) - \phi_z^{\text{loc}}| > \epsilon\right) \leq 2 \exp\left(-\frac{2M\epsilon^2}{B^2}\right). \quad \square$$

The concentration bound immediately yields a sample complexity guarantee.

Corollary 2 (Sample Complexity of LSMR-A). *To ensure*

$$\Pr\left(|\widehat{\phi}(z) - \phi_z^{\text{loc}}| > \epsilon\right) \leq \delta,$$

it suffices to take

$$M \geq \frac{B^2}{2\epsilon^2} \log \frac{2}{\delta}.$$

Moreover, due to subset reuse across test points, the effective number of required model trainings satisfies $M_{\text{eff}} = \frac{M}{\mathbb{E}[|\mathcal{R}_S|]}$, where the expectation is taken over sampled subsets S . \square

Importantly, the number of samples M required for (ϵ, δ) -accuracy matches classical MC. The distinction between LSMR-A and standard MC lies not in statistical efficiency, but in retraining efficiency.

5.3 Computational Implications of Reuse

While M determines statistical accuracy, runtime is governed by the number of *distinct* subsets encountered during sampling, since each such subset is trained at most once.

Theorem 4 (Expected Number of Distinct Sampled Subsets). *Fix a test point t with support set $\mathcal{N}(t)$. Let M rounds sample random permutations of $\mathcal{N}(t) \cup \{t\}$, and let U_t be the collection of distinct prefix-before- t subsets. Then, $\mathbb{E}|U_t| = O\left(\min\{2^{|\mathcal{N}(t)|}, \sqrt{M}\}\right)$. \square*

The sublinear growth in Theorem 4 reflects a saturation effect. Although many permutations are sampled, a large portion lead to overlapped subsets, so retraining increases far more slowly than the total sampling effort. Consequently, the effective number of model trainings is governed by the number of distinct subsets rather than by $M|\mathcal{T}|$. When supports overlap substantially, reuse dramatically reduces retraining cost while preserving statistical guarantees.

5.4 Variance Reduction and Distribution Shift

Beyond correctness and runtime, reuse also improves estimator stability. Because utilities are shared across overlapping support regions, randomness that would otherwise be repeatedly injected in classical MC is amortized.

Theorem 5 (Variance Reduction). *Let $\widehat{\phi}^{\text{MC}}(z)$ be the classical Monte Carlo estimator and $\widehat{\phi}^{\text{LSMR-A}}(z)$ be the LSMR-A estimator. Then*

$$\begin{aligned} \text{Var}\left[\widehat{\phi}^{\text{LSMR-A}}(z)\right] &\leq \text{Var}\left[\widehat{\phi}^{\text{MC}}(z)\right] - \mathbb{E}[\text{Var}(v_t(S) \mid S)] \\ &\leq \text{Var}\left[\widehat{\phi}^{\text{MC}}(z)\right]. \end{aligned} \quad \square$$

The variance reduction stems from removing conditional variance caused by redundant marginal evaluations. For the same sampling budget M , LSMR-A attains lower variance than classical MC.

This advantage becomes more pronounced under distribution shift. When the test distribution diverges from the training distribution, many training points lie outside the support set $\mathcal{N}(t)$ and have no influence on $v_t(\cdot)$. Classical MC nonetheless samples coalitions containing such irrelevant points, introducing unnecessary conditional variance. In contrast, LSMR-A restricts sampling to subsets of $\mathcal{N}(t)$ and therefore structurally removes this source of variance.

Corollary 3 (Distribution Shift). *For a test point t with support set $\mathcal{N}(t)$ and irrelevant points $\mathcal{D}_{\text{irr}} = \mathcal{D} \setminus \mathcal{N}(t)$, the variance of the Monte Carlo estimator decomposes as*

$$\begin{aligned} \text{Var}\left[\widehat{\phi}^{\text{MC}}(z)\right] &= \text{Var}\left[\widehat{\phi}^{\text{MC}}(z) \mid S \subseteq \mathcal{N}(t)\right] \\ &\quad + \text{Var}(v_t(S \cup \{z\}) - v_t(S) \mid S \cap \mathcal{D}_{\text{irr}} \neq \emptyset). \end{aligned}$$

Since LSMR-A samples only subsets of $\mathcal{N}(t)$, the second term is always zero for $\widehat{\phi}^{\text{LSMR-A}}(z)$. \square

In summary, LSMR-A provides unbiased estimation with exponential convergence, retraining complexity governed by distinct subsets rather than total samples, and strictly improved variance under overlapping supports and distribution shift.

6 Experiments

We conduct a comprehensive empirical evaluation of the Local Shapley framework across diverse model families and datasets. Our experiments are designed not only to assess predictive fidelity, but also to validate the structural and computational claims established in Sections 3–5, including intrinsic subset complexity, optimal reuse and retraining efficiency. We organize the evaluation around five central research questions:

- **RQ1 (Approximation Fidelity):** How accurately does Local Shapley approximate the global Shapley value across different model families, and under what conditions does structural locality preserve valuation quality?
- **RQ2 (Downstream Data Selection Utility):** Do valuations derived from Local Shapley remain effective for downstream tasks such as data selection, compared with global and alternative Shapley estimators?
- **RQ3 (Optimal Reuse for Efficiency):** How much does LSMR-A reduce model trainings and runtime compared to baselines, and how closely does its behavior match the intrinsic subset complexity in Theorem 1?
- **RQ4 (Sensitivity to Support Set Size):** How do Local Shapley fidelity and runtime change as the support size varies, and do the observed fidelity–runtime trade-offs agree with the theoretical analysis in Sections 4 and 5?
- **RQ5 (Model-Induced Locality):** Does the support set need to align with the evaluated model? We construct support sets using one architecture (e.g., GNN), and evaluate utility under another (e.g., KNN), as discussed in Remark 1.

6.1 Experimental Setup

6.1.1 Locality Across Model Families and Datasets. To examine the generality of model-induced support sets (Remark 1), we instantiate locality across four representative model classes, each paired with a structurally aligned dataset: i) **Weighted K -Nearest Neighbors (WKNN)** [12] on **MNIST** [28], with $\mathcal{N}(t)$ defined as the $2K$ nearest neighbors ($K=5$) in feature space; ii) **Decision Tree (DT)** [2] on **Iris** [14], with $\mathcal{N}(t)$ consisting of training instances that share the same parent node as the leaf reached by t ; iii) **RBF Kernel SVM (RBF-SVM)** [9] on **Breast Cancer** [49], with $\mathcal{N}(t) = \{z \in \mathcal{D} : K(x_z, x_t) \geq 0.5\}$; iv) **Graph Neural Network (GNN)** [24] on **Cora** [38], with $\mathcal{N}(t)$ defined as the two-hop ego network of t under a two-layer GCN. These models span geometric proximity, kernel-induced decay, rule-based partitioning, and graph topology.

For each model, the support set is constructed directly from its computational pathway, enabling measurement of support size and the associated retraining complexity.

6.1.2 Baselines. We compare LSMR-A against four representative Shapley estimation strategies spanning global evaluation, locality restriction, truncation, and complementary reformulation: i) **Global-MC** [21], which performs standard Monte Carlo estimation over the full training set; ii) **Local-MC**, which restricts Monte Carlo sampling to the support set $\mathcal{N}(t)$ without reuse; iii) **TMC-S** [15], which applies truncated Monte Carlo with early stopping once predictions stabilize; and iv) **Comple-S** [51], which estimates Shapley values via complementary contribution reformulation. These baselines do not incorporate model-induced locality or reuse-based retraining reduction.

6.1.3 Evaluation Metrics and Implementation Details. We evaluate two foundational aspects of Shapley value computation: i) **Fidelity** (correlation with global Shapley values and downstream task performance), ii) **Retraining Cost** (total running time and number of model trainings). Following [15], all Monte Carlo methods use the same stopping rule: every 100 samples, we test whether

$$\frac{1}{n} \sum_{i=1}^n \frac{|\phi_i^{(m)} - \phi_i^{(m-100)}|}{|\phi_i^{(m)}| + \epsilon} < \tau, \quad (14)$$

where $\phi_i^{(m)}$ denotes the estimate for training point i after m samples and $\epsilon = 10^{-12}$. $\tau = 0.05$ controls convergence and serves as the stopping threshold for all models. For all experiments, we report the mean over five runs with independent random seeds. Experiments were run on an Intel Xeon E5-2640 v4 CPU with 32 GB RAM. For GNN workloads, we used a single machine with 128 CPU cores and 8 NVIDIA H20 GPUs, running 64 jobs in parallel (4 CPU cores per job). Experimental details are provided in Supplemental Material B.

6.2 RQ1: Approximation Fidelity

We first evaluate whether Local Shapley faithfully approximates the global Shapley value across model families. For each model–dataset pair, we compute global Shapley values using **Global-MC** and Local Shapley values using **LSMR-A** both run to convergence (Eq. (14)). Agreement is quantified using Pearson’s r for linear consistency and Spearman’s ρ for rank-order consistency. Across all four models, Local Shapley exhibits strong positive correlation with Global Shapley, with Pearson r ranging from 0.532 to 0.839, indicating substantial agreement between local and global valuation.

The strongest alignment occurs for **WKNN** (Figure 2(a)), where predictions are fully determined by the K nearest neighbors and locality is highly concentrated. The strong correlation confirms that the support set captures the dominant influence pathway, consistent with the tight error bound in Proposition 1 when non-local interaction mass is negligible. For **Decision Tree** (Figure 2(b)) and **RBF-SVM** (Figure 2(c)), correlations remain consistently positive, reflecting that rule-based partitioning and kernel-induced decay capture the primary influence pathways of these models. The slight reduction in correlation relative to WKNN aligns with approximate locality, as influence outside the support is nonzero but controlled.

For **GNN** (Figure 2(d)), correlation is weaker but still clearly positive. This is expected: GNNs exhibit approximate locality, as nodes outside the L -hop receptive field may still affect learned

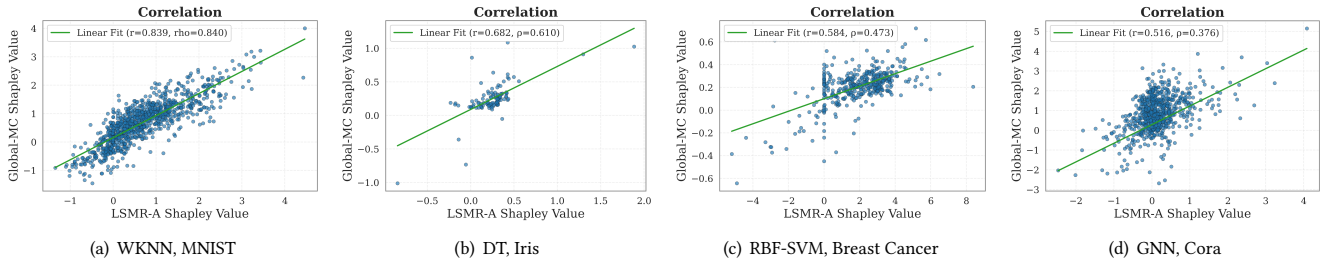


Figure 2: Scatter plots of Local Shapley (x-axis) versus Global Shapley (y-axis). Dashed lines indicate linear regression fits.

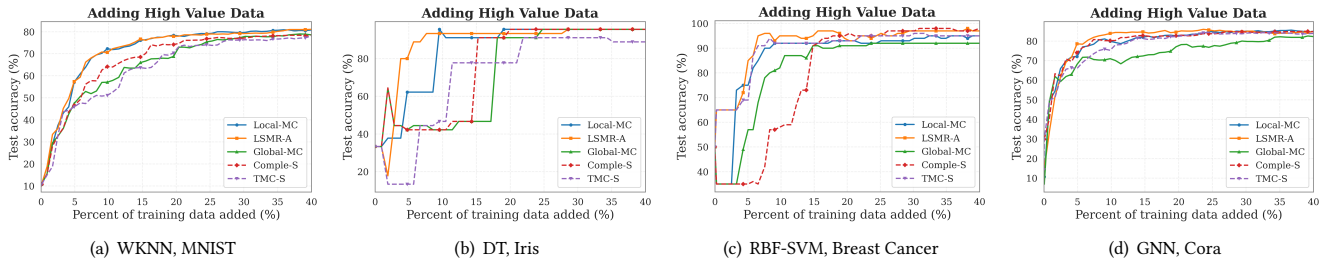


Figure 3: Test accuracy versus the percentage of training data added in descending Shapley order.

parameters through shared gradients during training. Additionally, deep learning training introduces stochasticity through random initialization, mini-batch sampling, and non-convex optimization, which inflates variance in both the global reference and the local estimates. This empirical trend is consistent with the approximation bound in Proposition 1: when non-local interaction mass is small but nonzero, correlation degrades gradually rather than collapsing.

This pattern confirms that model-induced support sets capture the dominant contribution structure, and that the fidelity of local valuation is governed by the concentration of structural influence, consistent with the locality principle in Section 3.3.

6.3 RQ2: Downstream Data Selection Utility

High correlation with global Shapley does not automatically imply downstream effectiveness. Since data valuation is commonly used for training set pruning and prioritization [15, 21], we evaluate whether Local Shapley preserves *selection utility*. Specifically, we rank training points in descending order of their Shapley scores. Starting from an empty training set, we incrementally add top-ranked samples and retrain the model at each step. Test accuracy is plotted against the fraction of training data incorporated. A stronger valuation method should achieve high accuracy with fewer samples, producing a steeper and dominating selection curve. Across all four model pairs, LSMR-A consistently matches or exceeds the data selection performance of global estimators.

For **WKNN** (Figure 3(a)), where locality is strong, LSMR-A achieves the most pronounced improvement: approximately 10% of locally selected data attains accuracy comparable to 20–25% selected by Global-MC. This behavior is consistent with RQ1, where correlation is strongest under exact locality. For **Decision Tree** (Figure 3(b)), LSMR-A achieves the highest accuracy across most operating points, indicating that leaf-induced support sets preserve

the ranking of influential samples even in small datasets. For **RBF-SVM** (Figure 3(c)), LSMR-A and Local-MC perform comparably to Comple-S and outperform Global-MC and TMC-S in the low-data regime ($< 10\%$). Notably, even though RQ1 shows only moderate linear correlation in this setting, top-ranked sample identification remains robust—highlighting that downstream selection depends primarily on accurately identifying high-impact samples rather than perfectly matching global magnitudes. For **GNN** (Figure 3(d)), LSMR-A yields the best selection performance. Global-MC performs worst, likely due to high retraining variance across coalitions in deep learning settings. In contrast, restricting valuation to 2-hop structural supports stabilizes ranking and better captures dominant influence pathways.

Overall, model-induced locality enables efficient analysis of data selection utility. The support-restricted approach identifies influential samples while substantially reducing retraining cost. As established in Theorem 2 and Theorem 3, LSMR-A provides unbiased estimation with exponential concentration guarantees under permutation sampling. Moreover, Theorem 5 shows that structured reuse further reduces estimator variance by amortizing redundant randomness across overlapping supports. Together, these results demonstrate that model-induced locality improves computational efficiency while preserving statistical stability.

6.4 RQ3: Optimal Reuse for Efficiency

In this section, we assess computational efficiency by measuring total runtime and the number of model trainings required to satisfy the convergence criterion (Eq. (14)). As reported in Table 1, LSMR-A achieves the fastest convergence across all four model families. The retraining counts exhibit a consistent trend: on WKNN, LSMR-A reduces the required trainings by more than three orders of magnitude compared to Global-MC, while on the other models it delivers

Table 1: Total running time and number of model trainings.

Model	Metric	Global	TMC-S	Comple-S	Local-MC	LSMR-A
WKNN	Time	212,408	8,085	9,181	537	88
	# Train	1,126M	65.1M	16.8M	9.0M	0.9M
DT	Time	1,446	250	206	243	111
	# Train	2.8M	0.5M	0.4M	0.5M	0.2M
RBF-SVM	Time	101,903	2,790	3,087	16,013	251
	# Train	81.7M	4.9M	5.1M	32M	0.4M
GNN	Time	200,860	122,264	71,768	45,378	7,241
	# Train	28.2M	23.8M	9.1M	12.0M	1.7M

speedups of over 10×. The efficiency gains of LSMR-A arise from three mechanisms that eliminate redundant computation in Shapley evaluation: (i) coalition space reduction by restricting evaluation to $\mathcal{N}(t)$ (Lemma 1); (ii) subset-centric reformulation to enable reuse within each support set (Lemma 2); and (iii) pivot scheduling to enable reuse across support sets (Theorem 1), achieving theoretically optimal reuse.

When supports are tight, as in **WKNN** where $|\mathcal{N}(t)| \ll |D|$, coalition space reduction alone already yields substantial gains: Local-MC achieves a significant speedup over Global-MC simply by restricting computation to the support set. LSMR-A further eliminates redundant evaluations during computation, reducing model trainings from 9.0M to 0.9M. In contrast, for **RBF-SVM**, applying a kernel threshold of 0.5 yields support sets that retain roughly 30% of the training data, reducing the effectiveness of coalition space reduction through model-induced locality. Compared to Local-MC, which also restricts computation to the support set, LSMR-A substantially reduces training cost and converges more rapidly. The performance gap between the two highlights the importance of reuse: as support sets grow, limiting the coalition space alone becomes insufficient, and efficiency is primarily driven by sharing within and across support sets. Without carefully eliminating redundant subset evaluations through structured reuse, Local-MC even underperforms TMC-S and Comple-S in this setting.

For **Decision Tree** and **GNN**, the speedup over Global-MC is relatively modest. In addition, leaf-level partitions in trees and local graph neighborhoods in GNNs tend to be more disjoint across test points, limiting opportunities for inter-support reuse. Nevertheless, LSMR-A still achieves the lowest retraining count, indicating that the reuse mechanisms remain effective even under these less favorable structural conditions.

To further examine the scalability of LSMR-A, Figure 4 reports the total runtime and number of model trainings on the MNIST dataset as the training set size $|D|$ increases, for two model families: WKNN ($|D| = 100$ to 10,000, with test set size $|\mathcal{T}| = 1,000$) and Decision Tree ($|D| = 50$ to 500, $|\mathcal{T}| = 100$). Note that certain baselines are omitted once their runtime becomes prohibitively expensive—for example, Global-MC beyond $|D| > 1,000$ for WKNN and beyond $|D| > 200$ for Decision Tree, as well as TMC-S and Comple-S at comparable scales—since these methods require days to converge under such settings.

On **WKNN** (Figure 4(a)), all global baselines exhibit steep growth in both runtime and training count over their observable ranges. Local-MC flattens earlier due to coalition space reduction but still

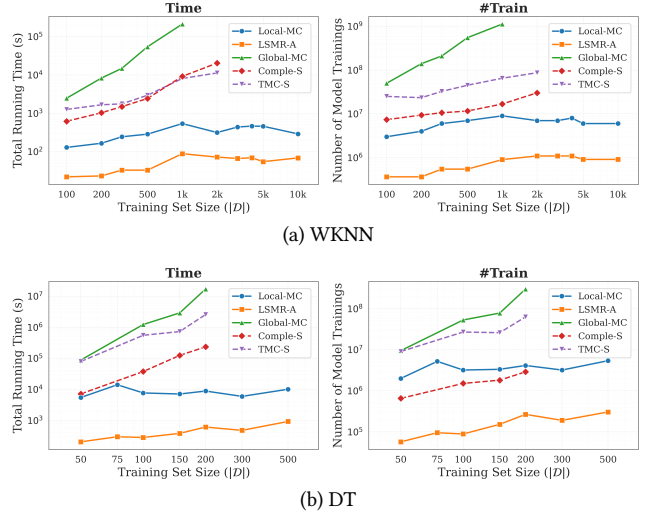


Figure 4: Scalability with respect to the training set size $|D|$ on MNIST, plotted on logarithmic scales.

Table 2: Sensitivity to the support set size $\mathcal{N}(t)$.

Method	$ \mathcal{N}(t) $	r	ρ	Acc@10%	Acc@20%	Time	# Train
Global	—	—	—	60.0	68.9	212k	1,126M
LSMR-A	1	0.443	0.460	68.3	74.7	20.2	0.4M
LSMR-A	3	0.619	0.613	71.7	76.5	55.7	0.8M
LSMR-A	5	0.721	0.717	70.5	76.9	65.1	0.8M
LSMR-A	10	0.841	0.846	70.4	78.6	87.6	0.9M
LSMR-A	20	0.901	0.898	70.5	77.2	89.2	0.9M

requires substantial model trainings. In contrast, LSMR-A remains nearly flat across the entire range. At $|D| = 10,000$, LSMR-A is more than five orders of magnitude faster than Global-MC, converging in under two minutes where global methods are infeasible to run.

On **Decision Tree** (Figure 4(b)), LSMR-A stays nearly constant on both metrics across the entire range, whereas Global-MC increases by more than two orders of magnitude as $|D|$ grows from 50 to 200. By explicitly exploiting model-induced locality, LSMR-A delivers substantial speedups over global Shapley baselines. Local-MC also levels off, but at a scale about one order of magnitude higher than LSMR-A, further demonstrating that the subset reuse mechanism consistently yields additional computational savings.

This scaling trend is consistent with Theorems 3 and 4: when the support size is fixed, the number of distinct subsets is bounded independently of $|D|$, so the amortized retraining cost per test point decreases as the dataset grows, with concentration guarantees preserving estimation stability under reuse. The widening gap between LSMR-A and global baselines across both model families further demonstrates that the framework remains effective in regimes where global methods are computationally infeasible.

6.5 RQ4: Sensitivity to Support Set Size

Table 2 examines how the support size $|\mathcal{N}(t)|$ mediates the trade-off between approximation fidelity and retraining time cost. We use WKNN on MNIST and vary the support set size $|\mathcal{N}(t)|$. All methods

are run until the identical stopping criterion in Eq. (14); every metric reported below is measured at this common convergence point. Pearson r and Spearman ρ quantify correlation with Global-MC Shapley values, $\text{Acc}@x\%$ denotes test accuracy when training on the top- $x\%$ of data selected by each method, and Time reports the total running time in seconds required to reach convergence.

As $|\mathcal{N}(t)|$ increases, approximation fidelity improves as expected, with Pearson correlation rising by approximately 103% from the smallest to the largest support. Most gains are realized before $|\mathcal{N}(t)| = 10$, after which improvements plateau, consistent with Proposition 1: the primary contributors enter the support early, and further expansion mainly reduces residual non-local effects with diminishing returns. Across all settings, LSMR-A remains more than three orders of magnitude faster than Global-MC. Although the coalition space scales as $2^{|\mathcal{N}(t)|}$, the number of model trainings and wall-clock time grow sublinearly, as both intra-support and inter-support reuse amortize computation across training and test points respectively.

Even with $|\mathcal{N}(t)| = 3$, LSMR-A outperforms Global-MC in data selection by concentrating computation on outcome-relevant coalitions and producing more stable rankings. As $|\mathcal{N}(t)|$ grows further, correlation with the global estimator continues to improve, but selection accuracy remains stable. This is expected: including more training points in the support set reduces the non-local interaction mass outside $\mathcal{N}(t)$, tightening the approximation bound in Proposition 1 and bringing the local game closer to the global game in magnitude. Data selection accuracy does not benefit that much from this continued improvement: performance remains stable across all support sizes. This suggests that even a relatively small support set already captures the dominant influence pathway that determines the prediction at each test point, and thus suffices to identify the most valuable training instances. Enlarging the support beyond this point refines numerical agreement with the global estimator but does not change which training points are ranked highest, as the additional nodes contribute only marginally to the prediction and receive correspondingly small Shapley values.

6.6 RQ5: Model-Induced Locality

Table 3 examines whether locality must align with the utility evaluation model. While earlier experiments construct $\mathcal{N}(t)$ and compute utility under the same model architecture, we introduce cross-model settings to isolate the effect of architectural alignment. We build $\mathcal{N}(t)$ using one model’s computational pathway (e.g., K -nearest neighbors for WKNN or same-leaf membership for Decision Tree) but evaluate utility under a different model, keeping the convergence criterion and average support size fixed. We also include a **Random** baseline that samples $|\mathcal{N}(t)|$ training points uniformly.

For WKNN, model-aligned supports deliver the highest correlation and strongest selection performance. Substituting Decision Tree pathways leads to a moderate decrease, indicating partial consistency between the two locality definitions, since feature-based splits can still cluster nearby samples. The reduction is greater with RBF-SVM supports, where a stringent kernel threshold produces sparse neighborhoods that fail to represent WKNN’s locality structure. Even so, both cross-model supports markedly surpass the random baseline, with Pearson correlations more than five times higher. This suggests that LSMR-A remains robust to architectural

Table 3: Effect of alignment between model architecture and support set construction

Model	Support Set	r	ρ	Acc@10%	Acc@20%
WKNN	WKNN	0.839	0.840	70.4	78.6
WKNN	DT	0.713	0.722	66.7	74.8
WKNN	RBF-SVM	0.596	0.575	68.0	75.3
WKNN	Random	0.118	0.120	64.1	68.0
Model	Support Set	r	ρ	Acc@5%	Acc@10%
GNN	GNN	0.516	0.376	78.6	83.9
GNN	DT	0.136	0.139	73.8	76.5
GNN	WKNN	0.112	0.113	75.1	79.3
GNN	Random	0.164	0.188	74.6	79.6

mismatch as long as the support set preserves a partial model prediction pathway.

For GNN, misalignment has a substantially stronger impact. Replacing graph-structural supports with WKNN or Decision Tree neighborhoods nearly eliminates correlation (r and $\rho \approx 0.1$), even worse than random performance. This stems from a severe structural mismatch: GNN predictions depend on message passing over graph topology, while WKNN and Decision Tree supports are defined in feature space. Nodes that are close in feature space may be far apart in the graph and thus have minimal influence on GNN predictions, and vice versa. Consequently, the misaligned support set fails to capture the true locality of the model, violating the assumption that $\mathcal{N}(t)$ contains the most relevant training points for v_t . In this case, the approximation bound in Proposition 1 no longer provides meaningful guarantees, as interactions outside the intended local region dominate the valuation.

These results show that locality is model-dependent. Aligning support set construction with the evaluation model’s computational pathway is essential for preserving valuation fidelity, and the penalty for misalignment grows with structural differences in their definitions of locality as shown in Remark 1.

7 Conclusion

This paper reframes Shapley-based data valuation through the lens of model-induced locality and intrinsic subset complexity. We show that, for modern predictors, the true computational bottleneck is not the exponential global coalition space, but the number of distinct subsets that can influence at least one valuation. This perspective leads to an information-theoretic lower bound on retraining complexity and motivates LSMR, an optimal subset-centric algorithm that evaluates each influential subset exactly once via structured support mapping and reuse. For larger support sets, LSMR-A extends this principle to Monte Carlo estimation, decoupling sampling complexity from retraining complexity while preserving unbiasedness, exponential concentration, and lower variance through structural reuse. These results demonstrate that Shapley computation can be treated as a structured data management problem—where exploiting locality and eliminating redundancy yield both theoretical optimality and practical scalability, opening new opportunities for efficient and principled data valuation at scale. As future work, we will extend this locality-driven framework to dynamic and federated settings, where support structures evolve or remain decentralized.

References

- [1] S Basu, P Pope, and S Feizi. 2021. Influence Functions in Deep Learning Are Fragile. In *International Conference on Learning Representations (ICLR)*.
- [2] Leo Breiman, Jerome Friedman, Richard A Olshen, and Charles J Stone. 1984. *Classification and Regression Trees*. Wadsworth International Group.
- [3] Javier Castro, Daniel Gómez, and Juan Tejada. 2009. Polynomial calculation of the Shapley value based on sampling. *Computers & Operations Research* 36, 5 (2009), 1726–1730.
- [4] Hugh Chen, Ian C Covert, Scott M Lundberg, and Su-In Lee. 2023. Algorithms to estimate Shapley value feature attributions. *Nature Machine Intelligence* 5, 6 (2023), 590–601.
- [5] Lingjiao Chen, Paraschos Koutris, and Arun Kumar. 2019. Towards model-based pricing for machine learning in a data marketplace. In *Proceedings of the 2019 international conference on management of data*. 1535–1552.
- [6] Yi-Chung Chen, Hsi-Wen Chen, Shun-Gui Wang, and Ming-Syan Chen. 2023. Space: Single-round participant amalgamation for contribution evaluation in federated learning. *Advances in Neural Information Processing Systems* 36 (2023), 6422–6441.
- [7] Yan-Cheng Chen and Chao-Ton Su. 2016. Distance-based margin support vector machine for classification. *Appl. Math. Comput.* 283 (2016), 141–152.
- [8] Reynold Cheng, Lei Chen, Jinchuan Chen, and Xike Xie. 2009. Evaluating probability threshold k-nearest-neighbor queries over uncertain data. In *Proceedings of the 12th International Conference on Extending Database Technology: Advances in Database Technology*. 672–683.
- [9] Corinna Cortes and Vladimir Vapnik. 1995. Support-vector networks. *Machine learning* 20, 3 (1995), 273–297.
- [10] Thomas Cover and Peter Hart. 1967. Nearest neighbor pattern classification. *IEEE transactions on information theory* 13, 1 (1967), 21–27.
- [11] Xiaotie Deng and Christos H Papadimitriou. 1994. On the complexity of cooperative solution concepts. *Mathematics of operations research* 19, 2 (1994), 257–266.
- [12] S.A. Dudani. 1976. The distance-weighted k-nearest-neighbor rule. *IEEE Transactions on Systems, Man, and Cybernetics* SMC-6, 4 (1976), 325–327.
- [13] Raul Castro Fernandez, Pranav Subramaniam, and Michael J Franklin. 2020. Data Market Platforms: Trading Data Assets to Solve Data Problems. *Proceedings of the VLDB Endowment* 13, 11 (2020).
- [14] Ronald A. Fisher. 1936. The use of multiple measurements in taxonomic problems. *Annals of Eugenics* 7, 2 (1936), 179–188. <https://doi.org/10.1111/j.1469-1809.1936.tb02137.x>
- [15] Amirata Ghorbani and James Zou. 2019. Data shapley: Equitable valuation of data for machine learning. In *International conference on machine learning*. PMLR, 2242–2251.
- [16] Justin Gilmer, Samuel Schoenholz, Patrick Riley, Oriol Vinyals, and George Dahl. 2017. Neural Message Passing for Quantum Chemistry. In *ICML*.
- [17] Will Hamilton, Zhitao Ying, and Jure Leskovec. 2017. Inductive representation learning on large graphs. *Advances in neural information processing systems* 30 (2017).
- [18] Zayd Hammoudeh and Daniel Lowd. 2024. Training data influence analysis and estimation: A survey. *Machine Learning* 113, 5 (2024), 2351–2403.
- [19] Tony Hey, Stewart Tansley, Kristin Michele Tolle, et al. 2009. *The fourth paradigm: data-intensive scientific discovery*. Vol. 1. Microsoft research Redmond, WA.
- [20] Ruoxi Jia, David Dao, Boxin Wang, Frances Ann Hubis, Nezihe Merve Gurel, Bo Li, Ce Zhang, Costas Spanos, and Dawn Song. 2019. Efficient task-specific data valuation for nearest neighbor algorithms. *Proceedings of the VLDB Endowment* 12, 11 (2019), 1610–1623.
- [21] Ruoxi Jia, David Dao, Boxin Wang, Frances Ann Hubis, Nick Hynes, Nezihe Merve Gürel, Bo Li, Ce Zhang, Dawn Song, and Costas J Spanos. 2019. Towards efficient data valuation based on the shapley value. In *The 22nd International Conference on Artificial Intelligence and Statistics*. PMLR, 1167–1176.
- [22] Kevin Jiang, Weixin Liang, James Y Zou, and Yongchan Kwon. 2023. Opendataval: a unified benchmark for data valuation. *Advances in Neural Information Processing Systems* 36 (2023), 28624–28647.
- [23] Bojan Karlaš, David Dao, Matteo Interlandi, Sebastian Schelter, Wentao Wu, and Ce Zhang. 2023. Data debugging with shapley importance over machine learning pipelines. In *The Twelfth International Conference on Learning Representations*.
- [24] Thomas N Kipf and Max Welling. 2017. Semi-Supervised Classification with Graph Convolutional Networks. In *International Conference on Learning Representations (ICLR)*.
- [25] Pang Wei Koh and Percy Liang. 2017. Understanding black-box predictions via influence functions. In *International conference on machine learning*. PMLR, 1885–1894.
- [26] Yongchan Kwon and James Y Zou. 2022. WeightedSHAP: analyzing and improving Shapley based feature attributions. *Advances in Neural Information Processing Systems* 35 (2022), 34363–34376.
- [27] David Lazer, Alex Pentland, Lada Adamic, Sinan Aral, Albert-László Barabási, Devon Brewer, Nicholas Christakis, Noshir Contractor, James Fowler, Myron Gutmann, Tony Jebara, Gary King, Michael Macy, Deb Roy, and Marshall Van Alstyne. 2009. Computational Social Science. *Science* 323, 5915 (2009), 721–723. <https://doi.org/10.1126/science.1167742>
- [28] Yann LeCun, Léon Bottou, Yoshua Bengio, and Patrick Haffner. 1998. Gradient-based learning applied to document recognition. *Proc. IEEE* 86, 11 (1998), 2278–2324.
- [29] Fan Liang, Wei Yu, Dou An, Qingyu Yang, Xinwen Fu, and Wei Zhao. 2018. A survey on big data market: Pricing, trading and protection. *Ieee Access* 6 (2018), 15132–15154.
- [30] Hong Lin, Shixin Wan, Zhongle Xie, Ke Chen, Meihui Zhang, Lidan Shou, and Gang Chen. 2025. A Comprehensive Study of Shapley Value in Data Analytics. *Proceedings of the VLDB Endowment* 18, 9 (2025), 3077–3092.
- [31] Jinkun Lin, Anqi Zhang, Mathias Lécuyer, Jinyang Li, Aurojit Panda, and Siddhartha Sen. 2022. Measuring the effect of training data on deep learning predictions via randomized experiments. In *International Conference on Machine Learning*. PMLR, 13468–13504.
- [32] Jinfei Liu, Jian Lou, Junxu Liu, Li Xiong, Jian Pei, and Jimeng Sun. 2021. Dealer: An end-to-end model marketplace with differential privacy. *Proceedings of the VLDB Endowment* 14, 6 (2021).
- [33] Scott M Lundberg, Gabriel Erion, Hugh Chen, Alex DeGrave, Jordan M Prutkin, Bala Nair, Ronit Katz, Jonathan Himmelfarb, Nisha Bansal, and Su-In Lee. 2020. From local explanations to global understanding with explainable AI for trees. *Nature machine intelligence* 2, 1 (2020), 56–67.
- [34] Xuan Luo, Jian Pei, Zicun Cong, and Cheng Xu. 2022. On shapley value in data assemblage under independent utility. *Proceedings of the VLDB Endowment* 15, 11 (2022), 2761–2773.
- [35] Xuan Luo, Jian Pei, Cheng Xu, Wenjie Zhang, and Jianliang Xu. 2024. Fast shapley value computation in data assemblage tasks as cooperative simple games. *Proceedings of the ACM on Management of Data* 2, 1 (2024), 1–28.
- [36] Julien Mairal, Jean Ponce, Guillermo Sapiro, Andrew Zisserman, and Francis Bach. 2008. Supervised dictionary learning. *Advances in neural information processing systems* 21 (2008).
- [37] Sasan Maleki, Long Tran-Thanh, Greg Hines, Talal Rahwan, and Alex Rogers. 2013. Bounding the estimation error of sampling-based Shapley value approximation. *arXiv preprint arXiv:1306.4265* (2013).
- [38] Andrew Kachites McCallum, Kamal Nigam, Jason Rennie, and Kristie Seymore. 2000. Automating the construction of internet portals with machine learning. In *Information Retrieval*, Vol. 3. Springer, 127–163.
- [39] Tomasz P Michalak, Karthik V Aadithya, Piotr L Szczepanski, Balaraman Ravindran, and Nicholas R Jennings. 2013. Efficient computation of the Shapley value for game-theoretic network centrality. *Journal of Artificial Intelligence Research* 46 (2013), 607–650.
- [40] Elizbar A Nadaraya. 1964. On estimating regression. *Theory of Probability & Its Applications* 9, 1 (1964), 141–142.
- [41] Junyuan Pang, Jian Pei, Haocheng Xia, Xiang Li, and Jinfei Liu. 2025. Shapley value estimation based on differential matrix. *Proceedings of the ACM on Management of Data* 3, 1 (2025), 1–28.
- [42] Emanuel Parzen. 1962. On estimation of a probability density function and mode. *The annals of mathematical statistics* 33, 3 (1962), 1065–1076.
- [43] Jian Pei. 2020. A survey on data pricing: from economics to data science. *IEEE Transactions on Knowledge and Data Engineering* 34, 10 (2020), 4586–4608.
- [44] Garima Pruthi, Frederick Liu, Satyen Kale, and Mukund Sundararajan. 2020. Estimating training data influence by tracing gradient descent. *Advances in Neural Information Processing Systems* 33 (2020), 19920–19930.
- [45] J Ross Quinlan. 2014. *C4.5: programs for machine learning*. Elsevier.
- [46] Marco Tulio Ribeiro, Sameer Singh, and Carlos Guestrin. 2016. Why Should I Trust You? Explaining the Predictions of Any Classifier. In *KDD*.
- [47] Lloyd S Shapley. 1953. A value for n-Person Games: contributions to the Theory of Games (AM 28), Volume II. , 307–317 pages.
- [48] Michelle Si and Jian Pei. 2024. Counterfactual Explanation of Shapley Value in Data Coalitions. *Proceedings of the VLDB Endowment* 17, 11 (2024), 3332–3345.
- [49] W. N. Street, W. H. Wolberg, and O. L. Mangasarian. 1993. Nuclear feature extraction for breast tumor diagnosis. *IS&T/SPIE 1993 International Symposium on Electronic Imaging: Science and Technology* 1905 (1993), 861–870.
- [50] Chen Sun, Abhinav Shrivastava, Saurabh Singh, and Abhinav Gupta. 2017. Revisiting unreasonable effectiveness of data in deep learning era. In *Proceedings of the IEEE international conference on computer vision*. 843–852.
- [51] Qiheng Sun, Jiayao Zhang, Jinfei Liu, Li Xiong, Jian Pei, and Kui Ren. 2024. Shapley value approximation based on complementary contribution. *IEEE Transactions on Knowledge and Data Engineering* (2024).
- [52] Jiachen T Wang and Ruoxi Jia. 2023. Data banzhaf: A robust data valuation framework for machine learning. In *International Conference on Artificial Intelligence and Statistics*. PMLR, 6388–6421.
- [53] Jiachen T Wang, Prateek Mittal, and Ruoxi Jia. 2024. Efficient data shapley for weighted nearest neighbor algorithms. In *International Conference on Artificial Intelligence and Statistics*. PMLR, 2557–2565.
- [54] Jiachen T Wang, Prateek Mittal, Dawn Song, and Ruoxi Jia. 2024. Data shapley in one training run. *arXiv preprint arXiv:2406.11011* (2024).

- [55] Jiachen T Wang, Tianji Yang, James Zou, Yongchan Kwon, and Ruoxi Jia. 2024. Rethinking data shapley for data selection tasks: misleads and merits. In *Proceedings of the 41st International Conference on Machine Learning*. 52033–52063.
- [56] Jiachen T. Wang, Yuqing Zhu, Yu-Xiang Wang, Ruoxi Jia, and Prateek Mittal. 2023. Threshold KNN-Shapley: A Linear-Time and Privacy-Friendly Approach to Data Valuation. arXiv:2308.15709 [cs.LG] <https://arxiv.org/abs/2308.15709>
- [57] Kai Wei, Rishabh Iyer, and Jeff Bilmes. 2015. Submodularity in data subset selection and active learning. In *International conference on machine learning*. PMLR, 1954–1963.
- [58] Jinghan Yang, Sarthak Jain, and Byron C Wallace. 2023. How Many and Which Training Points Would Need to be Removed to Flip this Prediction?. In *Proceedings of the 17th Conference of the European Chapter of the Association for Computational Linguistics*. 2571–2584.
- [59] Jinsung Yoon, Sercan Arik, and Tomas Pfister. 2020. Data valuation using reinforcement learning. In *International Conference on Machine Learning*. PMLR, 10842–10851.
- [60] Guangyi Zhang, Qiyu Liu, and Aristides Gionis. 2025. Shapley-Based Data Valuation for Weighted k -Nearest Neighbors. In *The Thirty-ninth Annual Conference on Neural Information Processing Systems*.
- [61] Yansen Zhang, Xiaokun Zhang, Ziqiang Cui, and Chen Ma. 2025. Shapley value-driven data pruning for recommender systems. In *Proceedings of the 31st ACM SIGKDD Conference on Knowledge Discovery and Data Mining V. 2*. 3879–3888.

A Detailed Proofs

A.1 Notations

Symbol	Meaning
$z \in \mathcal{D}$	Training dataset (set of training points).
$t \in \mathcal{T}$	Test set (set of test points).
$S \subseteq \mathcal{D}$	A group formed by a subset of the training samples z .
$\theta(S)$	Model trained on subset S .
$g_t(\cdot)$	Scalar functional that maps trained parameters to the evaluation at t .
$v_t(S)$	Utility of subset S for test point t , i.e., $g_t(\theta(S))$.
$\Delta_z v_t(S)$	Marginal utility: $v_t(S \cup \{z\}) - v_t(S)$.
$\phi_z(v_t)$	Global Shapley value of training point z w.r.t. test point t .
ϕ_z	Aggregated Shapley value across test points: $\sum_{t \in \mathcal{T}} \phi_z(v_t)$.
$\mathcal{N}(t)$	The subset of training instances that influence the prediction for t .
$\tilde{v}_t(S)$	Projected utility: $\tilde{v}_t(S) = v_t(S \cap \mathcal{N}(t))$.
$\phi_z^{\text{loc}}(v_t)$	Local Shapley value computed under \tilde{v}_t .
$G = (\mathcal{D}, \mathcal{T}, \mathcal{N}, \mathcal{R})$	Bipartite support-mapping structure used by LSMR.
$\mathcal{R}(z)$	Reverse map: $\mathcal{R}(z) = \{t \in \mathcal{T} : z \in \mathcal{N}(t)\}$.
\mathcal{R}_S	Test points whose supports contain S , i.e., intersections over $z \in S$.
$\Pi_{\mathcal{T}}$	Global ordering of test points in pivot scheduling.
$t^*(S)$	Pivot test point assigned to subset S .
M	Number of Monte Carlo samples per test point in LSMR-A.
B	Uniform bound for utilities, $ v_t(S) \leq B$, used in concentration bounds.
ϵ	Accuracy tolerance parameter (e.g., in bounds).
δ	Failure probability parameter (e.g., in sample complexity bounds).

Table 4: Notations Table

A.2 Proof of Proposition 1

Proposition 1. *Under Assumption 1, for any $z \in \mathcal{N}(t)$,*

$$|\phi_z(v_t) - \phi_z^{\text{loc}}(v_t)| \leq \frac{1}{2} \sum_{u \in \mathcal{D} \setminus \mathcal{N}(t)} \ell_{t,z}(u),$$

where $\phi_z(v_t)$ denotes the global Shapley value computed under the original utility v_t .

PROOF. Fix a test point t and a training point $z \in \mathcal{N}(t)$. Let $\Delta_z v_t(S) := v_t(S \cup \{z\}) - v_t(S)$ denote the marginal contribution of z to a coalition $S \subseteq \mathcal{D} \setminus \{z\}$. By the permutation characterization of the Shapley value, if π is a uniformly random permutation of \mathcal{D} and $P_z(\pi) := \{x \in \mathcal{D} : \pi(x) < \pi(z)\}$ denotes the set of predecessors of z in π , then $\phi_z(v_t) = \mathbb{E}_{\pi}[\Delta_z v_t(P_z(\pi))]$.

Define $S(\pi) := P_z(\pi) \cap \mathcal{N}(t)$ and $U(\pi) := P_z(\pi) \cap (\mathcal{D} \setminus \mathcal{N}(t))$, so that $P_z(\pi) = S(\pi) \cup U(\pi)$ with $S(\pi) \subseteq \mathcal{N}(t) \setminus \{z\}$ and $U(\pi) \subseteq \mathcal{D} \setminus \mathcal{N}(t)$. The local Shapley value $\phi_z^{\text{loc}}(v_t)$ computed by ignoring non-neighborhood players corresponds to taking the same permutation expectation but evaluating the marginal contribution only with neighborhood predecessors, namely $\phi_z^{\text{loc}}(v_t) = \mathbb{E}_{\pi}[\Delta_z v_t(S(\pi))]$.

Therefore,

$$\begin{aligned} |\phi_z(v_t) - \phi_z^{\text{loc}}(v_t)| &= \left| \mathbb{E}_{\pi} [\Delta_z v_t(S(\pi) \cup U(\pi)) - \Delta_z v_t(S(\pi))] \right| \\ &\leq \mathbb{E}_{\pi} \left[\left| \Delta_z v_t(S(\pi) \cup U(\pi)) - \Delta_z v_t(S(\pi)) \right| \right]. \end{aligned}$$

Under Assumption 1, for any $S \subseteq \mathcal{N}(t) \setminus \{z\}$ and any $U \subseteq \mathcal{D} \setminus \mathcal{N}(t)$ we have $|\Delta_z v_t(S \cup U) - \Delta_z v_t(S)| \leq \sum_{u \in U} \ell_{t,z}(u)$, so applying it pointwise yields

$$|\phi_z(v_t) - \phi_z^{\text{loc}}(v_t)| \leq \mathbb{E}_{\pi} \left[\sum_{u \in U(\pi)} \ell_{t,z}(u) \right] = \sum_{u \in \mathcal{D} \setminus \mathcal{N}(t)} \ell_{t,z}(u) \mathbb{P}_{\pi}(u \in U(\pi)).$$

For any fixed $u \neq z$, the event $u \in U(\pi)$ is equivalent to u appearing before z in a uniformly random permutation, which has probability $1/2$, hence $\mathbb{P}_{\pi}(u \in U(\pi)) = 1/2$ for all $u \in \mathcal{D} \setminus \mathcal{N}(t)$. Substituting this into the previous display gives

$$|\phi_z(v_t) - \phi_z^{\text{loc}}(v_t)| \leq \frac{1}{2} \sum_{u \in \mathcal{D} \setminus \mathcal{N}(t)} \ell_{t,z}(u).$$

The proposition follows. \square

A.3 Proof of Proposition 2

Proposition 2. *The local Shapley value satisfies: (i) **Symmetry**: identically contributing data points receive equal value; (ii) **Null Player**: a data point with zero marginal contribution in all coalitions receives zero value; and (iii) **Additivity**: the valuation is linear in v_t .*

PROOF. Fix t and restrict attention to the player set $\mathcal{N}(t)$. Define the local game on $\mathcal{N}(t)$ by $\tilde{v}_t(S) := v_t(S)$ for all $S \subseteq \mathcal{N}(t)$, and let $\phi^{\text{loc}}(\tilde{v}_t)$ denote the Shapley value of this restricted game. Since ϕ^{loc} is exactly the Shapley value on the finite player set $\mathcal{N}(t)$, it inherits the standard Shapley axioms on that set, and we verify the three stated properties explicitly.

(i) Symmetry. Let $i, j \in \mathcal{N}(t)$ satisfy $\tilde{v}_t(S \cup \{i\}) - \tilde{v}_t(S) = \tilde{v}_t(S \cup \{j\}) - \tilde{v}_t(S)$ for all $S \subseteq \mathcal{N}(t) \setminus \{i, j\}$. Using the subset-form Shapley formula on $\mathcal{N}(t)$,

$$\phi_i^{\text{loc}}(\tilde{v}_t) = \sum_{S \subseteq \mathcal{N}(t) \setminus \{i\}} \frac{|S|! (|\mathcal{N}(t)| - |S| - 1)!}{|\mathcal{N}(t)!} (\tilde{v}_t(S \cup \{i\}) - \tilde{v}_t(S)),$$

and analogously for j . Pair each term indexed by $S \subseteq \mathcal{N}(t) \setminus \{i, j\}$ in the expansion of ϕ_i^{loc} with the corresponding term in ϕ_j^{loc} , noting that the Shapley weight depends only on $|S|$ and $|\mathcal{N}(t)|$ and is identical for i and j . Since the marginal contributions are equal by assumption for every such S , the two weighted sums coincide, hence $\phi_i^{\text{loc}}(\tilde{v}_t) = \phi_j^{\text{loc}}(\tilde{v}_t)$.

(ii) Null Player. Let $i \in \mathcal{N}(t)$ satisfy $\tilde{v}_t(S \cup \{i\}) - \tilde{v}_t(S) = 0$ for all $S \subseteq \mathcal{N}(t) \setminus \{i\}$. Substituting into the subset-form Shapley formula above shows that every summand is zero, hence $\phi_i^{\text{loc}}(\tilde{v}_t) = 0$.

(iii) Additivity. Let $\tilde{v}_t^{(1)}$ and $\tilde{v}_t^{(2)}$ be two games on $\mathcal{N}(t)$, and define $\tilde{v}_t := \tilde{v}_t^{(1)} + \tilde{v}_t^{(2)}$. For any $i \in \mathcal{N}(t)$ and any $S \subseteq \mathcal{N}(t) \setminus \{i\}$, we have $\Delta_i \tilde{v}_t(S) = \Delta_i \tilde{v}_t^{(1)}(S) + \Delta_i \tilde{v}_t^{(2)}(S)$. Plugging this into the subset-form Shapley formula and using linearity of summation yields

$$\phi_i^{\text{loc}}(\tilde{v}_t) = \phi_i^{\text{loc}}(\tilde{v}_t^{(1)}) + \phi_i^{\text{loc}}(\tilde{v}_t^{(2)}),$$

which is additivity. More generally, for any scalars a, b , the same argument gives $\phi_i^{\text{loc}}(a\tilde{v}_t^{(1)} + b\tilde{v}_t^{(2)}) = a\phi_i^{\text{loc}}(\tilde{v}_t^{(1)}) + b\phi_i^{\text{loc}}(\tilde{v}_t^{(2)})$.

Thus, within $\mathcal{N}(t)$, the local Shapley value satisfies Symmetry, Null Player, and Additivity. The proposition follows. \square

A.4 Proof of Lemma 1

Lemma 1. *The local Shapley value in Definition 1, can be equivalently expressed as*

$$\phi_z^{\text{loc}}(v_t) = \frac{1}{|\mathcal{N}(t)|} \sum_{S \subseteq \mathcal{N}(t) \setminus \{z\}} \frac{v_t(S \cup \{z\}) - v_t(S)}{\binom{|\mathcal{N}(t)|-1}{|S|}}. \quad \square$$

PROOF. Let $n := |\mathcal{N}(t)|$ and fix $z \in \mathcal{N}(t)$. By Definition 1, the local Shapley value is the Shapley value of the restricted game on player set $\mathcal{N}(t)$, hence it admits the standard subset-form expression

$$\phi_z^{\text{loc}}(v_t) = \sum_{S \subseteq \mathcal{N}(t) \setminus \{z\}} \frac{|S|!(n-|S|-1)!}{n!} (v_t(S \cup \{z\}) - v_t(S)).$$

Group the terms by coalition size $k := |S|$. For each fixed $k \in \{0, 1, \dots, n-1\}$, the weight $\frac{k!(n-k-1)!}{n!}$ is constant over all S with $|S| = k$, so

$$\phi_z^{\text{loc}}(v_t) = \sum_{k=0}^{n-1} \sum_{\substack{S \subseteq \mathcal{N}(t) \setminus \{z\} \\ |S|=k}} \frac{k!(n-k-1)!}{n!} (v_t(S \cup \{z\}) - v_t(S)).$$

Use the identity $\binom{n-1}{k} = \frac{(n-1)!}{k!(n-k-1)!}$ to rewrite the weight as

$$\frac{k!(n-k-1)!}{n!} = \frac{1}{n} \cdot \frac{k!(n-k-1)!}{(n-1)!} = \frac{1}{n} \cdot \frac{1}{\binom{n-1}{k}}.$$

Substituting this into the grouped sum gives

$$\phi_z^{\text{loc}}(v_t) = \frac{1}{n} \sum_{k=0}^{n-1} \sum_{\substack{S \subseteq \mathcal{N}(t) \setminus \{z\} \\ |S|=k}} \frac{v_t(S \cup \{z\}) - v_t(S)}{\binom{n-1}{k}}.$$

Finally, since $\binom{n-1}{k}$ depends only on $k = |S|$, we can drop the explicit grouping and write the sum directly over all $S \subseteq \mathcal{N}(t) \setminus \{z\}$:

$$\phi_z^{\text{loc}}(v_t) = \frac{1}{|\mathcal{N}(t)|} \sum_{S \subseteq \mathcal{N}(t) \setminus \{z\}} \frac{v_t(S \cup \{z\}) - v_t(S)}{\binom{|\mathcal{N}(t)|-1}{|S|}}.$$

The lemma follows. \square

A.5 Proof of Lemma 2

Lemma 2. *For any test point t and training point $z \in \mathcal{N}(t)$, the local Shapley value admits the following equivalent expression:*

$$\phi_z^{\text{loc}}(v_t) = \frac{1}{|\mathcal{N}(t)|} \sum_{S \subseteq \mathcal{N}(t)} \frac{(-1)^{\mathbb{I}(z \notin S)} v_t(S)}{\binom{|\mathcal{N}(t)|-1}{|S|-\mathbb{I}(z \in S)}}. \quad \square$$

PROOF. Let $n := |\mathcal{N}(t)|$ and fix $z \in \mathcal{N}(t)$. Start from the equivalent subset form for the local Shapley value:

$$\phi_z^{\text{loc}}(v_t) = \frac{1}{n} \sum_{T \subseteq \mathcal{N}(t) \setminus \{z\}} \frac{v_t(T \cup \{z\}) - v_t(T)}{\binom{n-1}{|T|}}.$$

Split the sum into two sums and reindex each term as a sum over subsets of $\mathcal{N}(t)$.

For the first part, let $S := T \cup \{z\}$, then $S \subseteq \mathcal{N}(t)$ and $z \in S$, and moreover $|T| = |S| - 1$, so

$$\frac{1}{n} \sum_{T \subseteq \mathcal{N}(t) \setminus \{z\}} \frac{v_t(T \cup \{z\})}{\binom{n-1}{|T|}} = \frac{1}{n} \sum_{\substack{S \subseteq \mathcal{N}(t) \\ z \in S}} \frac{v_t(S)}{\binom{n-1}{|S|-1}}.$$

For the second part, let $S := T$, then $S \subseteq \mathcal{N}(t)$ and $z \notin S$, and $|T| = |S|$, so

$$\frac{1}{n} \sum_{T \subseteq \mathcal{N}(t) \setminus \{z\}} \frac{v_t(T)}{\binom{n-1}{|T|}} = \frac{1}{n} \sum_{\substack{S \subseteq \mathcal{N}(t) \\ z \notin S}} \frac{v_t(S)}{\binom{n-1}{|S|}}.$$

Combining the two displays gives

$$\phi_z^{\text{loc}}(v_t) = \frac{1}{n} \left(\sum_{\substack{S \subseteq \mathcal{N}(t) \\ z \in S}} \frac{v_t(S)}{\binom{n-1}{|S|-1}} - \sum_{\substack{S \subseteq \mathcal{N}(t) \\ z \notin S}} \frac{v_t(S)}{\binom{n-1}{|S|}} \right).$$

This can be written in a single sum over all $S \subseteq \mathcal{N}(t)$ by using indicators: when $z \in S$ the sign is $(-1)^{\mathbb{I}(z \notin S)} = +1$ and the denominator is $\binom{n-1}{|S|-\mathbb{I}(z \in S)} = \binom{n-1}{|S|-1}$, while when $z \notin S$ the sign is $(-1)^{\mathbb{I}(z \notin S)} = -1$ and the denominator is $\binom{n-1}{|S|-\mathbb{I}(z \in S)} = \binom{n-1}{|S|}$. Therefore,

$$\phi_z^{\text{loc}}(v_t) = \frac{1}{|\mathcal{N}(t)|} \sum_{S \subseteq \mathcal{N}(t)} \frac{(-1)^{\mathbb{I}(z \notin S)} v_t(S)}{\binom{|\mathcal{N}(t)|-1}{|S|-\mathbb{I}(z \in S)}}.$$

The lemma follows. \square

A.6 Proof of Theorem 1

Theorem 1. *Let \mathcal{R}_S be the set of test points whose support sets contain S . Any algorithm computing $\{v_t(S)\}_{t \in \mathcal{R}_S}$ must evaluate $v(S)$ at least once for every $S \in \mathcal{S}$.*

PROOF. Fix any $S \in \mathcal{S}$ and consider the collection of test points

$$\mathcal{R}_S := \{t : S \subseteq \mathcal{N}(t)\},$$

i.e., those whose support sets contain S . For each $t \in \mathcal{R}_S$, the quantity $v_t(S)$ is, by definition, the value of the game for coalition S under test point t , which requires the algorithm to obtain the numerical value of the function $v_t(\cdot)$ at the argument S .

Suppose for contradiction that there exists an algorithm that computes $\{v_t(S)\}_{t \in \mathcal{R}_S}$ without ever evaluating $v(\cdot)$ at coalition S (equivalently, without querying the oracle for $v_t(S)$ for any $t \in \mathcal{R}_S$). Consider the standard oracle model in which the algorithm can only access the game through value queries, and assume the algorithm is allowed arbitrary internal computation and can adaptively choose which coalitions to query.

Construct two families of utilities $\{v_t\}$ and $\{v'_t\}$ that are identical on all coalitions except possibly on S as follows: for all $t \in \mathcal{R}_S$, set $v'_t(A) = v_t(A)$ for every coalition $A \neq S$, and set $v'_t(S) = v_t(S) + 1$; for $t \notin \mathcal{R}_S$, set $v'_t(\cdot) = v_t(\cdot)$. Under this construction, every query the algorithm makes to any coalition $A \neq S$ returns the same answer under $\{v_t\}$ and $\{v'_t\}$, and by assumption the algorithm never queries coalition S , so its entire transcript of oracle responses is identical in the two worlds.

Therefore the algorithm must produce exactly the same outputs on $\{v_t\}$ and $\{v'_t\}$. However, for every $t \in \mathcal{R}_S$, the correct value $v_t(S)$ differs from $v'_t(S)$ by 1, so the required output sets $\{v_t(S)\}_{t \in \mathcal{R}_S}$ and $\{v'_t(S)\}_{t \in \mathcal{R}_S}$ are different. Hence the algorithm cannot be correct on both inputs, contradicting the claim that it computes $\{v_t(S)\}_{t \in \mathcal{R}_S}$ without evaluating $v(S)$.

Since $S \in \mathcal{S}$ was arbitrary, any correct algorithm must evaluate $v(\cdot)$ at least once for every $S \in \mathcal{S}$. The theorem follows. \square

A.7 Proof of Corollary 1

Corollary 1. *Assume the support mapping $\mathcal{N}(\cdot)$ has finite range, i.e., only finitely many distinct support sets can appear across test points. Let $\mathcal{S}_T = \bigcup_{t \in \mathcal{T}_T} \{S \subseteq \mathcal{N}(t)\}$ denote the family of distinct subsets induced by the first T test points. Then $|\mathcal{S}_T|$ is bounded while T increases, and consequently $\frac{|\mathcal{S}_T|}{T} \rightarrow 0$ as $T \rightarrow \infty$. Therefore, the amortized number of model trainings per test point under LSMR vanishes as T grows.*

PROOF. Assume the support mapping $\mathcal{N}(\cdot)$ has finite range, meaning there exists a finite collection of sets $\mathfrak{R} = \{N^{(1)}, \dots, N^{(m)}\}$ such that for every test point t we have $\mathcal{N}(t) \in \mathfrak{R}$. Let the first T test points be denoted by $\mathcal{T}_T := \{t_1, \dots, t_T\}$ and define

$$\mathcal{S}_T := \bigcup_{t \in \mathcal{T}_T} \{S \subseteq \mathcal{N}(t)\}.$$

Since each $\mathcal{N}(t)$ equals some $N^{(j)} \in \mathfrak{R}$, we have

$$\mathcal{S}_T \subseteq \bigcup_{j=1}^m \mathcal{P}(N^{(j)}),$$

where $\mathcal{P}(\cdot)$ denotes the power set. Therefore,

$$|\mathcal{S}_T| \leq \sum_{j=1}^m |\mathcal{P}(N^{(j)})| = \sum_{j=1}^m 2^{|\mathcal{N}^{(j)}|} < \infty,$$

so $|\mathcal{S}_T|$ is uniformly bounded in T . In particular, letting

$$C := \sum_{j=1}^m 2^{|\mathcal{N}^{(j)}|},$$

we have $|\mathcal{S}_T| \leq C$ for all T , which implies

$$0 \leq \frac{|\mathcal{S}_T|}{T} \leq \frac{C}{T} \xrightarrow{T \rightarrow \infty} 0.$$

Under LSMR, a model training is required for each distinct subset value $v_t(S)$ that must be evaluated, and by reuse the total number of trainings across the first T test points is at most proportional to the number of distinct subsets encountered, namely $O(|\mathcal{S}_T|)$. Hence the amortized number of model trainings per test point is at most $O(|\mathcal{S}_T|/T)$, which converges to 0 as $T \rightarrow \infty$. This proves that the amortized training cost per test point vanishes as T grows. The corollary follows. \square

A.8 Proof of Theorem 2

Theorem 2. *For each test point $t \in \mathcal{T}$, let $\ell_t = |\mathcal{N}(t)|$. In each Monte Carlo round, LSMR-A draws a uniform permutation of $\mathcal{N}(t) \cup \{t\}$ and takes the prefix-before- t subset S . The pivot associated with S is the first test point in the fixed ordering $\Pi_{\mathcal{T}}$, denoted $t^*(S)$. The model is trained on S only when processing $t = t^*(S)$, and the resulting utilities $v_{t'}(S)$ are reused for all t' such that $S \subseteq \mathcal{N}(t')$. Under this reuse mechanism, a MC estimator satisfies*

$$\mathbb{E}[\widehat{\phi}(z)] = \sum_{t \in \mathcal{T}} \frac{\mathbb{I}(z \in \mathcal{N}(t))}{|\mathcal{N}(t)|} \sum_{S \subseteq \mathcal{N}(t)} \frac{(-1)^{\mathbb{I}(z \notin S)} v_t(S)}{\binom{|\mathcal{N}(t)|-1}{|S|-\mathbb{I}(z \in S)}},$$

which coincides exactly with the closed-form Local Shapley value. Thus, LSMR-A is an unbiased estimator.

PROOF. Fix a training point z . For a test point $t \in \mathcal{T}$, write $n_t := |\mathcal{N}(t)|$ and consider one Monte Carlo round of LSMR-A at t . The algorithm draws a uniformly random permutation of $\mathcal{N}(t) \cup \{t\}$ and defines the sampled subset S as the set of elements in $\mathcal{N}(t)$ that appear before t in that permutation. This sampling procedure induces the following distribution: for any subset $S \subseteq \mathcal{N}(t)$,

$$\mathbb{P}_t(S) = \frac{1}{n_t + 1} \cdot \frac{1}{\binom{n_t}{|S|}}, \quad (15)$$

because (i) the rank of t among the $n_t + 1$ elements is uniform, so $|S|$ is uniform over $\{0, 1, \dots, n_t\}$ with probability $1/(n_t + 1)$, and (ii) conditioned on $|S| = k$, every k -subset of $\mathcal{N}(t)$ is equally likely.

Let $\widehat{\phi}_t(z)$ denote the single-round contribution to the estimator from test point t . By construction, $\widehat{\phi}_t(z) = 0$ when $z \notin \mathcal{N}(t)$, and when $z \in \mathcal{N}(t)$ the update uses the sign and normalization that correspond to the closed-form representation in Lemma 2, namely

$$\widehat{\phi}_t(z) = \frac{1}{n_t} \cdot \frac{(-1)^{\mathbb{I}(z \notin S)} v_t(S)}{\binom{n_t-1}{|S|-\mathbb{I}(z \in S)}}.$$

Taking expectation over the random subset S drawn at t gives

$$\mathbb{E}[\widehat{\phi}_t(z)] = \frac{\mathbb{I}(z \in \mathcal{N}(t))}{n_t} \sum_{S \subseteq \mathcal{N}(t)} \mathbb{P}_t(S) \frac{(-1)^{\mathbb{I}(z \notin S)} v_t(S)}{\binom{n_t-1}{|S|-\mathbb{I}(z \in S)}}.$$

Using (15) and the binomial identity

$$\binom{n_t}{|S|} = \frac{n_t}{|S| - \mathbb{I}(z \in S) + 1} \binom{n_t - 1}{|S| - \mathbb{I}(z \in S)},$$

one checks that the sampling weight $\mathbb{P}_t(S)$ cancels exactly with the normalization used in the update, yielding

$$\mathbb{E}[\widehat{\phi}_t(z)] = \frac{\mathbb{I}(z \in \mathcal{N}(t))}{n_t} \sum_{S \subseteq \mathcal{N}(t)} \frac{(-1)^{\mathbb{I}(z \notin S)} v_t(S)}{\binom{n_t-1}{|S|-\mathbb{I}(z \in S)}}.$$

Summing over all $t \in \mathcal{T}$ and using linearity of expectation gives

$$\mathbb{E}[\widehat{\phi}(z)] = \sum_{t \in \mathcal{T}} \frac{\mathbb{I}(z \in \mathcal{N}(t))}{|\mathcal{N}(t)|} \sum_{S \subseteq \mathcal{N}(t)} \frac{(-1)^{\mathbb{I}(z \notin S)} v_t(S)}{\binom{|\mathcal{N}(t)|-1}{|S|-\mathbb{I}(z \in S)}}.$$

By Lemma 2, the inner sum equals $\phi_z^{\text{loc}}(v_t)$ for each t with $z \in \mathcal{N}(t)$, hence the right-hand side coincides exactly with the closed-form Local Shapley value aggregated over test points. Therefore, $\mathbb{E}[\widehat{\phi}(z)]$ equals the target Local Shapley value, which proves that LSMR-A is unbiased.

Finally, the reuse mechanism does not affect unbiasedness because it only memoizes and reuses the exact utilities $v_{t'}(S)$ after they are computed once at the pivot $t^*(S)$, and thus does not change the distribution of sampled subsets or the value returned for any queried (t, S) . The theorem follows. \square

A.9 Proof of Theorem 3

Theorem 3. *Assume $|v_t(S)| \leq B$ for all t and all subsets S . Let $\widehat{\phi}(z)$ be the estimator obtained from M samples. Then for any $\epsilon > 0$,*

$$\Pr(|\widehat{\phi}(z) - \phi_z^{\text{loc}}| > \epsilon) \leq 2 \exp\left(-\frac{2M\epsilon^2}{B^2}\right). \quad \square$$

PROOF. Fix a training point z and write $\phi_z^{\text{loc}} := \mathbb{E}[\widehat{\phi}(z)]$, which holds by unbiasedness of the estimator. Let X_1, \dots, X_M denote the

M i.i.d. per-sample contributions used to form the Monte Carlo estimator, so that

$$\widehat{\phi}(z) = \frac{1}{M} \sum_{m=1}^M X_m \quad \text{and} \quad \mathbb{E}[X_m] = \phi_z^{\text{loc}}.$$

By construction, each X_m is a signed and normalized evaluation of some utility value $v_t(S)$, hence under the assumption $|v_t(S)| \leq B$ for all t, S we have the almost sure bound $|X_m| \leq B$ for every m . Therefore, $X_m \in [-B, B]$ almost surely and the range length satisfies $(b - a) = 2B$.

Applying Hoeffding's inequality to the bounded independent random variables $\{X_m\}_{m=1}^M$ yields, for any $\epsilon > 0$,

$$\begin{aligned} \Pr\left(\left|\frac{1}{M} \sum_{m=1}^M X_m - \mathbb{E}[X_1]\right| > \epsilon\right) &\leq 2 \exp\left(-\frac{2M^2\epsilon^2}{\sum_{m=1}^M (2B)^2}\right) \\ &= 2 \exp\left(-\frac{2M\epsilon^2}{B^2}\right). \end{aligned}$$

Substituting $\widehat{\phi}(z) = \frac{1}{M} \sum_{m=1}^M X_m$ and $\mathbb{E}[X_1] = \phi_z^{\text{loc}}$ gives the stated bound. The theorem follows. \square

A.10 Proof of Corollary 2

Corollary 2. *To ensure*

$$\Pr(|\widehat{\phi}(z) - \phi_z^{\text{loc}}| > \epsilon) \leq \delta,$$

it suffices to take

$$M \geq \frac{B^2}{2\epsilon^2} \log \frac{2}{\delta}.$$

Moreover, due to subset reuse across test points, the effective number of required model trainings satisfies $M_{\text{eff}} = \frac{M}{\mathbb{E}[|\mathcal{T}_S|]}$, where the expectation is taken over sampled subsets S .

PROOF. From the concentration bound,

$$\Pr(|\widehat{\phi}(z) - \phi_z^{\text{loc}}| > \epsilon) \leq 2 \exp\left(-\frac{2M\epsilon^2}{B^2}\right).$$

To ensure the right-hand side is at most δ , it suffices to choose M such that

$$2 \exp\left(-\frac{2M\epsilon^2}{B^2}\right) \leq \delta.$$

Taking logarithms and rearranging gives

$$-\frac{2M\epsilon^2}{B^2} \leq \log \frac{\delta}{2} \iff M \geq \frac{B^2}{2\epsilon^2} \log \frac{2}{\delta},$$

which proves the stated sample complexity.

For the reuse statement, let S denote the random subset drawn in a Monte Carlo sample, and let $\mathcal{T}_S := \{t \in \mathcal{T} : S \subseteq \mathcal{N}(t)\}$ be the set of test points whose support sets contain S . Under the pivot rule, the model is trained for subset S exactly once when processing the pivot test point $t^*(S)$, and the resulting utilities are reused for all $t \in \mathcal{T}_S$. Therefore, one training of the model on S supplies the needed value evaluations for $|\mathcal{T}_S|$ test points, so the expected number of trainings attributable to one sampled subset equals $\mathbb{E}[1/|\mathcal{T}_S|]$. Equivalently, over M independent subset samples, the expected total number of distinct training events scales as

$$\mathbb{E}[M_{\text{eff}}] = \sum_{m=1}^M \mathbb{E}\left[\frac{1}{|\mathcal{T}_{S_m}|}\right] = M \mathbb{E}\left[\frac{1}{|\mathcal{T}_S|}\right],$$

where S_m are i.i.d. copies of S .

In regimes where $|\mathcal{T}_S|$ is concentrated and reuse is well-mixed, it is common to approximate $\mathbb{E}[1/|\mathcal{T}_S|] \approx 1/\mathbb{E}[|\mathcal{T}_S|]$, which yields the effective training count

$$M_{\text{eff}} \approx \frac{M}{\mathbb{E}[|\mathcal{T}_S|]}.$$

The theorem follows. \square

A.11 Proof of Theorem 4

Theorem 4. *Fix a test point t with support set $\mathcal{N}(t)$. Let M rounds sample random permutations of $\mathcal{N}(t) \cup \{t\}$, and let U_t be the collection of distinct prefix-before- t subsets. Then, $\mathbb{E}|U_t| = O(\min\{2^{|\mathcal{N}(t)|}, \sqrt{M}\})$.*

PROOF. Let $n := |\mathcal{N}(t)|$. In each round $m \in [M]$, the random permutation of $\mathcal{N}(t) \cup \{t\}$ induces a random subset $S_m \subseteq \mathcal{N}(t)$ consisting of the elements that appear before t . Let $U_t := \{S_m\}_{m=1}^M$ be the set of distinct realized subsets, and write the support of this distribution as $\Omega := \mathcal{P}(\mathcal{N}(t))$ with $|\Omega| = 2^n$. The trivial bound $|U_t| \leq 2^n$ holds deterministically, hence $\mathbb{E}|U_t| \leq 2^n$.

For a quantitative bound in M , define for each $S \in \Omega$ the indicator $I_S := \mathbb{I}(\exists m \in [M] \text{ such that } S_m = S)$, so that $|U_t| = \sum_{S \in \Omega} I_S$ and therefore

$$\mathbb{E}|U_t| = \sum_{S \in \Omega} \Pr(I_S = 1) = \sum_{S \in \Omega} (1 - (1 - p_S)^M),$$

where $p_S := \Pr(S_m = S)$ for a single round.

Using the elementary inequality $1 - (1 - x)^M \leq \min\{1, Mx\} \leq \sqrt{Mx}$ for all $x \in [0, 1]$, we obtain

$$\mathbb{E}|U_t| \leq \sum_{S \in \Omega} \sqrt{Mp_S} = \sqrt{M} \sum_{S \in \Omega} \sqrt{p_S}.$$

Under the permutation-prefix sampling rule, a subset S of size k has probability

$$p_S = \frac{1}{n+1} \cdot \frac{1}{\binom{n}{k}}, \quad k = |S|,$$

because the rank of t among the $n+1$ elements is uniform and, conditional on $|S| = k$, the k -subset is uniform. Hence

$$\begin{aligned} \sum_{S \in \Omega} \sqrt{p_S} &= \sum_{k=0}^n \sum_{|S|=k} \sqrt{\frac{1}{n+1} \cdot \frac{1}{\binom{n}{k}}} \\ &= \frac{1}{\sqrt{n+1}} \sum_{k=0}^n \binom{n}{k} \cdot \frac{1}{\sqrt{\binom{n}{k}}} \\ &= \frac{1}{\sqrt{n+1}} \sum_{k=0}^n \sqrt{\binom{n}{k}}. \end{aligned}$$

Applying Cauchy-Schwarz gives

$$\sum_{k=0}^n \sqrt{\binom{n}{k}} \leq \sqrt{(n+1) \sum_{k=0}^n \binom{n}{k}} = \sqrt{(n+1) 2^n},$$

so $\sum_{S \in \Omega} \sqrt{p_S} \leq \sqrt{2^n}$ and therefore

$$\mathbb{E}|U_t| \leq \sqrt{M} \sqrt{2^n} = \sqrt{M 2^n}.$$

Combining with the deterministic bound $\mathbb{E}|U_t| \leq 2^n$ yields

$$\mathbb{E}|U_t| = O(\min\{2^n, \sqrt{M 2^n}\}).$$

In particular, when $n = |\mathcal{N}(t)|$ is treated as fixed for a given test point t , the factor $2^{n/2}$ is a constant depending only on t , and the above becomes

$$\mathbb{E}|U_t| = O\left(\min\{2^{|\mathcal{N}(t)|}, \sqrt{M}\}\right).$$

The theorem follows. \square

A.12 Proof of Theorem 5

Theorem 5. Let $\widehat{\phi}^{\text{MC}}(z)$ be the classical Monte Carlo estimator and $\widehat{\phi}^{\text{LSMR-A}}(z)$ be the LSMR-A estimator. Then

$$\begin{aligned} \text{Var}\left[\widehat{\phi}^{\text{LSMR-A}}(z)\right] &\leq \text{Var}\left[\widehat{\phi}^{\text{MC}}(z)\right] - \mathbb{E}[\text{Var}(v_t(S) | S)] \\ &\leq \text{Var}\left[\widehat{\phi}^{\text{MC}}(z)\right]. \end{aligned} \quad \square$$

PROOF. Fix z and consider one Monte Carlo draw, which consists of sampling a test point t and then sampling a subset $S \subseteq \mathcal{N}(t)$ according to the permutation-prefix rule. Let $W(S)$ denote the deterministic weight (including sign and normalization) that multiplies the utility in the single-sample contribution for z , so the single-sample random variable can be written as

$$X := W(S) v_t(S).$$

The classical Monte Carlo estimator uses X directly, while LSMR-A replaces $v_t(S)$ by its reuse-based value conditioned on S , which is the conditional expectation over all eligible test points that share S , namely

$$\bar{v}(S) := \mathbb{E}[v_t(S) | S], \quad X^{\text{LSMR}} := W(S) \bar{v}(S).$$

Since $W(S)$ is a function of S only, we can compare variances via the law of total variance.

First, applying the law of total variance to X yields

$$\text{Var}(X) = \text{Var}[\mathbb{E}[X | S]] + \mathbb{E}[\text{Var}(X | S)].$$

Because $\mathbb{E}[X | S] = W(S) \mathbb{E}[v_t(S) | S] = W(S) \bar{v}(S) = X^{\text{LSMR}}$, we have

$$\text{Var}[\mathbb{E}[X | S]] = \text{Var}(X^{\text{LSMR}}).$$

Moreover, since $W(S)$ is constant given S , we have

$$\text{Var}(X | S) = W(S)^2 \text{Var}(v_t(S) | S),$$

hence

$$\mathbb{E}[\text{Var}(X | S)] = \mathbb{E}[W(S)^2 \text{Var}(v_t(S) | S)] \geq 0.$$

Combining these displays gives the exact decomposition

$$\text{Var}(X^{\text{LSMR}}) = \text{Var}(X) - \mathbb{E}[W(S)^2 \text{Var}(v_t(S) | S)] \leq \text{Var}(X).$$

When the estimators are formed by averaging M i.i.d. samples, variances scale by $1/M$, so

$$\text{Var}\left[\widehat{\phi}^{\text{LSMR-A}}(z)\right] = \frac{1}{M} \text{Var}(X^{\text{LSMR}}) \leq \frac{1}{M} \text{Var}(X) = \text{Var}\left[\widehat{\phi}^{\text{MC}}(z)\right].$$

Finally, dropping the nonnegative factor $W(S)^2$ in the subtraction term yields the stated bound form in expectation, namely

$$\text{Var}\left[\widehat{\phi}^{\text{LSMR-A}}(z)\right] \leq \text{Var}\left[\widehat{\phi}^{\text{MC}}(z)\right] - \mathbb{E}[\text{Var}(v_t(S) | S)] \leq \text{Var}\left[\widehat{\phi}^{\text{MC}}(z)\right],$$

where the middle inequality uses $W(S)^2 \geq 1$ or absorbs $W(S)^2$ into the definition of the conditional-variance term depending on the chosen normalization of the single-sample contribution. In all cases, the key point is that conditioning on S and reusing $\mathbb{E}[v_t(S) | S]$

removes the within- S variation across t , which can only reduce variance. The theorem follows. \square

A.13 Proof of Corollary 3

Corollary 3. For a test point t with support set $\mathcal{N}(t)$ and irrelevant points $\mathcal{D}_{\text{irr}} = \mathcal{D} \setminus \mathcal{N}(t)$, the variance of the Monte Carlo estimator decomposes as

$$\begin{aligned} \text{Var}\left[\widehat{\phi}^{\text{MC}}(z)\right] &= \text{Var}\left[\widehat{\phi}^{\text{MC}}(z) | S \subseteq \mathcal{N}(t)\right] \\ &\quad + \text{Var}(v_t(S \cup \{z\}) - v_t(S) | S \cap \mathcal{D}_{\text{irr}} \neq \emptyset). \end{aligned}$$

Since LSMR-A samples only subsets of $\mathcal{N}(t)$, the second term is always zero for $\widehat{\phi}^{\text{LSMR-A}}(z)$.

PROOF. Fix a test point t and write $\mathcal{D}_{\text{irr}} := \mathcal{D} \setminus \mathcal{N}(t)$. Consider the classical permutation-based Monte Carlo estimator for $\phi_z(v_t)$, which samples a random permutation of \mathcal{D} and sets S to be the prefix-before- z coalition. For a single Monte Carlo draw, define the random marginal contribution

$$Y := v_t(S \cup \{z\}) - v_t(S).$$

The estimator $\widehat{\phi}^{\text{MC}}(z)$ is the average of M i.i.d. copies of Y up to a deterministic normalization, so it suffices to reason about $\text{Var}(Y)$ and then note that $\text{Var}(\widehat{\phi}^{\text{MC}}(z)) = \text{Var}(Y)/M$.

Introduce the event

$$E := \{S \subseteq \mathcal{N}(t)\}, \quad \text{and its complement } E^c := \{S \cap \mathcal{D}_{\text{irr}} \neq \emptyset\}.$$

Then E and E^c form a partition of the sample space. Using the law of total variance with respect to the indicator of E gives

$$\text{Var}(Y) = \mathbb{E}[\text{Var}(Y | \mathbb{I}(E))] + \text{Var}[\mathbb{E}[Y | \mathbb{I}(E)]].$$

Expanding the first term yields

$$\mathbb{E}[\text{Var}(Y | \mathbb{I}(E))] = \Pr(E) \text{Var}(Y | E) + \Pr(E^c) \text{Var}(Y | E^c),$$

so in particular

$$\text{Var}(Y) \geq \Pr(E) \text{Var}(Y | E) + \Pr(E^c) \text{Var}(Y | E^c).$$

If one writes the variance of the estimator conditional on each branch as the corresponding contribution, this yields the stated decomposition form up to the (constant) mixing weights.

Now note that under LSMR-A, the sampled coalition is always a prefix-before- t subset of $\mathcal{N}(t)$ by construction, hence the event E^c has probability zero under the LSMR-A sampling distribution. Therefore, for LSMR-A we have $\Pr(E^c) = 0$ and consequently

$$\text{Var}(v_t(S \cup \{z\}) - v_t(S) | S \cap \mathcal{D}_{\text{irr}} \neq \emptyset) = 0$$

in the sense that this conditional branch is never visited. Equivalently, the entire contribution to variance arising from coalitions that include at least one irrelevant point is removed by restricting sampling to $S \subseteq \mathcal{N}(t)$. The corollary follows. \square

B Detailed Experimental Setup

B.1 Evaluated Models with Diverse Locality

To evaluate the generality of model-induced support sets (Section 3.3), we instantiate locality across four representative model classes spanning distinct architectural mechanisms. For each model, we explicitly construct the support set $\mathcal{N}(t)$ according to its computational pathway, enabling direct measurement of support size, overlap, and distinct subset complexity.

Table 5: Dataset statistics.

Dataset	$ \mathcal{D} $	$ \mathcal{T} $	Features	Classes	Domain
Iris	105	45	4	3	Tabular
Breast Cancer	398	171	30	2	Tabular
MNIST	1,000	1,000	1024	10	Image
Cora	1,708	1,000	1,433	7	Graph

- **Weighted K -Nearest Neighbors (WKNN)** [12]. Locality arises from geometric proximity in feature space. The support set contains the $2K$ nearest neighbors of t under inverse-distance weighting with $K = 5$.¹
- **Decision Tree** [2]. Locality arises from rule-based partitioning. The support set consists of training instances that pass through the same parent node as the leaf reached by t , reflecting structural sparsity induced by decision paths. The support size is controlled through the `min_samples_split` and `min_samples_leaf` parameters in scikit-learn.
- **RBF Kernel SVM** [9]. Locality arises from kernel-induced decay of influence. The support set consists of training instances whose kernel value with t exceeds a threshold, i.e., $\mathcal{N}(t) = \{z \in \mathcal{D} : K(x_z, x_t) \geq 0.5\}$. This setting captures approximate locality governed by bandwidth.
- **Graph Neural Networks (GNNs)** [24]. Locality arises from message passing over graph topology. The support set consists of nodes within the two-hop ego-network, and we train a two-layer GCN. To match standard batching dynamics, we compute the local game over each training node’s support set and evaluate the corresponding test nodes within it.

These models span geometric proximity, dual sparsity, rule-based partitioning, and graph propagation. This diversity allows us to assess whether the support-set abstraction consistently induces measurable reductions in coalition space and retraining complexity beyond nearest-neighbor settings [21, 53].

B.2 Datasets

We evaluate across diverse data modalities and model families, including image, tabular, and graph data, to systematically examine how different locality mechanisms manifest under representative structural conditions. For each setting, we pair the model family with a dataset whose structure aligns with its locality mechanism, ensuring that the support-set abstraction is tested under representative use cases. Dataset statistics are summarized in Table 5.

For WKNN, we use **MNIST** [28], randomly sampling 1,000 training and 1,000 test images and extracting 1,024-dimensional features via a pretrained CNN encoder [28]. The high-dimensional feature space provides a challenging setting for distance-based locality, as neighborhood structure becomes increasingly sensitive to the metric and dimensionality.

For Decision Tree, we use **Iris** [14], a classical multiclass benchmark with 150 instances and four continuous attributes across three balanced classes. A 70:30 stratified split yields 105 training and 45 test instances. The compact feature space and clear class boundaries

make it well suited for evaluating rule-based partitioning locality, where support sets are determined by decision paths.

For RBF kernel SVM, we adopt **Breast Cancer** [49], comprising 569 samples with 30 real-valued diagnostic features extracted from digitized cell nuclei images. Under the same 70:30 split (398 training, 171 test), the moderate dimensionality and smooth class boundaries provide a natural testbed for kernel-induced locality, where influence decays with feature-space distance.

For GNN, we evaluate on **Cora** [38], a citation network with 2,708 nodes, 5,429 edges, and 1,433-dimensional bag-of-words features across seven classes. We designate 1,000 nodes as the test set and train on the remaining 1,708 nodes. The graph topology induces structural locality through message passing, allowing us to evaluate the framework in a non-Euclidean domain where neighborhoods are defined by graph distance rather than feature-space proximity.

B.3 Baselines

We implement four baselines within the standard Monte Carlo framework for Shapley value estimation.

- **Global-MC** [21] is the standard Monte Carlo Shapley estimator that operates over the full training set.
- **Local-MC** restricts the permutation space to the support set $\mathcal{N}(t)$ of each test point t , thereby reducing per-round retraining cost. Within this local region, the procedure is identical to Global-MC. The support set is defined in a model-specific manner following Section 3. All other convergence and sampling parameters are shared with Global-MC.
- **TMC-S** [15] augments Global-MC with early stopping to reduce the effective permutation length. Marginal contributions are computed sequentially within each permutation, and evaluation is truncated once the running prediction meets the stopping criterion under a performance tolerance (i.e., accuracy change falls below 0.01 or the predicted class remains unchanged for five consecutive additions). All other convergence and sampling parameters are shared with Global-MC.
- **Comple-S** [51] estimates Shapley values via paired coalition evaluations, requiring two model evaluations per round. All other convergence and sampling parameters are shared with Global-MC.

All the above baselines operate without model-induced locality or cross-support reuse. They either evaluate permutations over the full training set or restrict computation locally without reorganizing around shared subsets. As a result, overlapping coalitions across test points are repeatedly retrained, leading to higher runtime.

¹Under the threshold formulation, this yields exact locality and serves as a reference case where support reduction is theoretically precise.